Article

Response Adjustability Analysis of Partial and Ordinary Differential Coupling System for Visco-Elastomer Sandwich Plate Coupled with Distributed Masses under Random Excitation via Spatial Periodicity Strategy

Zu-Guang Ying [1,*], **Zhi-Gang Ruan** [1] **and Yi-Qing Ni** [2]

1   Department of Mechanics, School of Aeronautics and Astronautics, Zhejiang University,
    Hangzhou 310027, China
2   Hong Kong Branch of National Rail Transit Electrification and Automation Engineering Technology Research
    Center, Department of Civil and Environmental Engineering, The Hong Kong Polytechnic University,
    Kowloon, Hong Kong
*   Correspondence: yingzg@zju.edu.cn

Abstract: Vibration control of composite structures coupled with distributed masses under random excitations is a significant issue. In this paper, partial and ordinary differential coupling equations are obtained from a periodic sandwich plate coupled with supported masses under random excitation. An analytical solution to the coupling equations is proposed, and the stochastic response adjustability of the system with various periodic distributions of geometrical and physical parameters is studied. Spatial periodic layer thickness and core modulus of the sandwich plate are considered based on the active-passive periodicity strategy. The periodically distributed masses are supported on the plate by coupling springs and dampers. Partial and ordinary differential coupling equations for the system including the periodic sandwich plate and supported masses are derived and then converted into unified ordinary differential equations for multi-mode coupling vibration. Generalized system stiffness, damping and mass are functions of the periodic parameters. Expressions of frequency response function and response spectral density of the system are obtained. Numerical results show the response adjustability via the spatially periodic geometrical and physical parameters. The results have the potential for application to dynamic control or optimization of sandwich structure systems.

Keywords: partial and ordinary differential coupling system; random vibration; sandwich plate; periodic distribution parameters; periodically distributed masses; spatial periodicity strategy

1. Introduction

Stochastic system vibration control is a significant issue in structural engineering. For example, vibration-sensitive instruments are supported on a base structure, and their vibration control has been presented [1]. Complex environmental disturbances are random excitations. The vibration control includes a design in the space and time domain. Most works presented are on the temporal control design, while relatively few works are on the spatial control design due to the challenge [2–7]. The spatial control design can include composite construction and configuration.

In terms of construction, damping sandwich structures have been designed to attenuate vibration. A sandwich plate with distributed masses was presented as a model for vibration-sensitive instruments supported on a planar structure under random excitation [1]. Because the vibration control performance of sandwich structures with non-adjustable viscoelastic cores is limited under various excitations, smart materials such as magneto-rheological liquid are considered to be the cores of sandwich structures, which are controllable by applied magnetic fields. However, the magneto-rheological liquid has

certain instability including magnetic particle settlement. Thus, a controllable magneto-rheological visco-elastomer has been proposed to replace the magneto-rheological liquid as the cores of sandwich structures [8].

A sandwich plate with a magneto-rheological visco-elastomer core has been studied; areas of investigation have included vibration and sound transmission characteristics [9–14], stochastic vibration responses [15], optimum location of partial cores [16,17] and dynamic stability [18,19]. However, in the research, the sandwich plate with a magneto-rheological visco-elastomer core was considered only as having uniform or locally uniform mechanical properties. Thus, to fully utilize the visco-elastomer spatial controllability, the configuration design of a sandwich plate with non-uniform or optimally distributed dynamic properties of visco-elastomer cores needs to be studied further. Accordingly, structural physical parameters have spatially non-uniform distribution and then structural dynamics differ from the conventional dynamics.

In terms of configuration, periodic structures which have spatially periodic distribution parameters studied exhibit special dynamic characteristics [20,21]. The periodicity design is applicable for improving sandwich structure dynamics. The periodic sandwich structure will have visco-elastomer dynamic properties spatially adjustable only by, for example, applied magnetic fields, but the configuration remains unchanged, which is considered an active spatial periodicity strategy. Geometrical periodicity design is considered a passive spatial periodicity strategy. Therefore, periodic sandwich plates with visco-elastomer cores controlled spatially need to be studied further for dynamic optimization or vibration control based on the active–passive spatial periodicity strategy.

On the other hand, the actual connection between the plate and supported masses is not fully fixed, and the masses have responses unequal to the supporting points of the plate. Thus, the connection relation needs to be considered, and it generally is described by spring and damper forces which are characterized by coupling stiffness and damping. That is, the coupling stiffness and damping between the sandwich structure and supported masses are considered to take into account mass dynamics. Therefore, the periodic sandwich plate coupled with distributed supported masses under random excitation results in the system dynamics which are described by ordinary and partial differential coupling equations with space-varying parameters and random excitation. More modes need to be used in the analysis because conventional vibration modes are coupled with periodic distribution parameters. To explore the adjustable system dynamics, a direct numerical solution to the parameter-varying equations with random excitation is unsuitable for stochastic response statistics under various spatial parameters. An analytical solution to the equations is an alternative [22–27]. Therefore, the analysis method and dynamics adjustability of the partial and ordinary differential coupling system for the visco-elastomer sandwich plate coupled with supported masses under random excitation through spatial periodicity strategy need to be studied further for dynamic optimization or vibration control.

In the present study, a class of controllable visco-elastomers such as the magneto-rheological visco-elastomer is considered as the core of a sandwich plate. The visco-elastomer sandwich plate coupled with distributed masses is used as a model for vibration-sensitive instruments supported on a planar structure. Partial and ordinary differential coupling equations are derived from the periodic sandwich plate coupled with supported masses under random excitation. Stochastic response characteristics of the coupling system are studied, where geometrical and physical parameters have various spatially periodic distributions based on active–passive periodicity strategy and the masses are distributed periodically. First, the layer thickness and core modulus of the sandwich plate are considered as periodic distributions in the plate plane. The distributed masses are supported on the sandwich plate by coupling springs and dampers. Partial and ordinary differential coupling equations for transverse and longitudinal coupling motions of the system including the periodic sandwich plate and supported masses are derived. Second, an analytical solution method is proposed. The partial differential equations are firstly converted into ordinary differential equations for multi-mode coupling vibration of the system according to the

Galerkin method. The system equations are unified with ordinary differential coupling equations. Then, expressions of frequency response function and response spectral density of the system are obtained by using stochastic dynamics theory. Finally, the influences of the periodic geometrical and physical parameters and distributed masses with coupling stiffness and damping on stochastic response characteristics of the system are shown by numerical results.

2. Partial and Ordinary Differential Coupling Equations for Spatially Periodic Sandwich Plate Coupled with Supported Masses under Random Excitation

A class of controllable visco-elastomers such as the magneto-rheological visco-elastomer is used as the core of a sandwich plate. The visco-elastomer sandwich plate coupled with distributed masses is used as a model of a coupling structural system for vibration-sensitive instruments supported on a planar structure. The connection between the plate and masses is not fully fixed, and thus the supported masses are considered as coupled with the plate by springs and dampers. Periodic parameter distribution of the sandwich plate is adopted to improve dynamic characteristics and adjust vibration response. Facial layer thickness is designed as a spatially periodic distribution based on a passive strategy. The spatially periodic distribution of core layer modulus is adjusted by external control action such as an applied magnetic field based on an active strategy. The visco-elastomer (with adjustable dynamics) sandwich plate coupled with supported masses is shown in Figure 1, where the facial layer thickness and core layer modulus are spatially periodic functions (varying with coordinates x and y), and the supported masses are distributed periodically. The length and width of the plate are a (in the x direction) and b (in the y direction), respectively. Facial layers have identical Young's modulus E_1, Poisson's ratio μ, mass density ρ_1 and thickness h_1. The core layer has mass density ρ_2 and thickness h_2. The kth supported mass has mass $m_{mk} = m_{0k} \times ab$, but its size is neglected due to the parameter being small compared with the plate length and width. The stiffness of the kth coupling spring is $k_{mk} = k_{0k} \times ab$ and the damping of the kth coupling damper is $c_{mk} = c_{0k} \times ab$, by which the kth supported mass is coupled with the plate. The sandwich plate is under a support motion excitation. The support has transverse displacement w_0 which is a random disturbance.

The basic assumptions of the sandwich plate are as follows: (1) the facial layer material is isotropic while the core material is transversely isotropic under external action (e.g., magneto-rheological visco-elastomer under applied magnetic fields) along coordinate z; (2) normal stresses of the core layer are small and neglected; (3) normal stresses of the facial layers in the z direction are small and neglected; (4) transverse displacement of the sandwich plate is invariant with coordinate z; (5) the cross-section of each facial layer is perpendicular to its axis line, and cross-section of the core layer remains in the plane during deformation; (6) longitudinal and rotational inertias of the plate are small and neglected; (7) interfaces between the facial layers and core layer are continuous all the time [15]. The visco-elastomer core has adjustable dynamic properties including damping and stiffness [9–19]. The Young's modulus of the core is neglected because it is much smaller than that of the facial layers. Shearing deformation of the core layer is larger than that of the facial layers and is considered. Based on viscoelastic dynamic stress–strain relation [28], shear stresses τ_{2xz} (on cross section (x,z)) and τ_{2yz} (on cross section (y,z)) of the core layer are expressed by the corresponding shear strains γ_{2xz} and γ_{2yz} as

$$\tau_{2xz} = G_{2a}\gamma_{2xz} + G_{2c}\frac{\partial\gamma_{2xz}}{\partial t} \tag{1}$$

$$\tau_{2yz} = G_{2a}\gamma_{2yz} + G_{2c}\frac{\partial\gamma_{2yz}}{\partial t} \tag{2}$$

where t is the time variable, and modulus parameters G_{2a} and G_{2c} are adjustable by actively external control action. The modulus parameters designed vary periodically with coordinates x and y and are expressed as
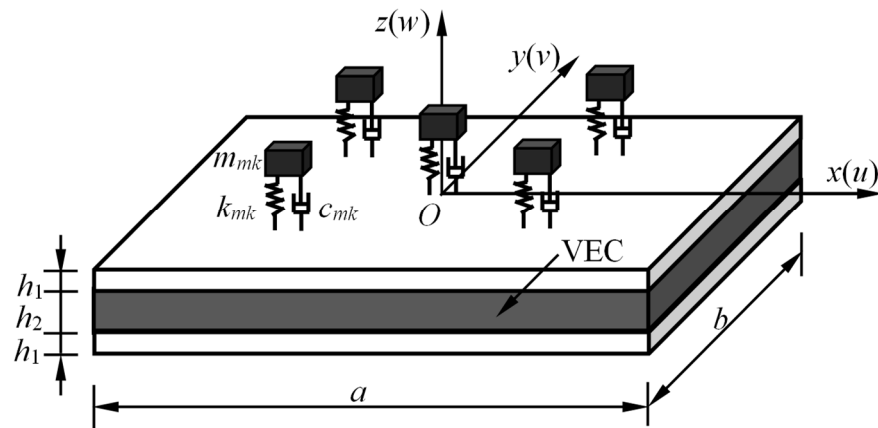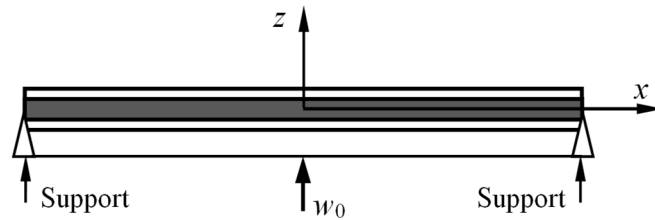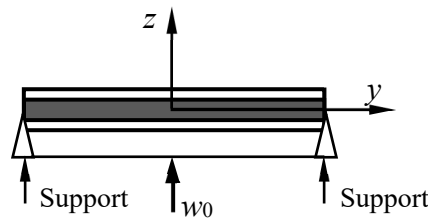
(**a**) Sandwich plate with masses

(**b**) Boundary simply supported plate under support excitation w_0 in xz-plane

(**c**) Boundary simply supported plate under support excitation w_0 in yz-plane

Figure 1. Sandwich plate with visco-elastomer core (VEC) and elastically supported masses under support excitation.

$$G_{2a}(x, y) = e_{a1} + b_{a1} \cos \frac{2k_a \pi x}{a} \cos \frac{2k_b \pi y}{b} \tag{3}$$

$$G_{2c}(x, y) = e_{c1} + b_{c1} \cos \frac{2k_a \pi x}{a} \cos \frac{2k_b \pi y}{b} \tag{4}$$

where e_{a1} and e_{c1} are non-periodic parts of the shear modulus parameters G_{2a} and G_{2c}, respectively; b_{a1} and b_{c1} are wave amplitudes of periodic parts of the shear modulus parameters; and k_a and k_b are wave numbers of periodic parts of the shear modulus parameters. The shear modulus of the core layer is periodic and adjustable based on an active spatial periodicity strategy. The active spatial strategy aims to determine optimal wave amplitudes and wave numbers of the shear modulus. Moreover, the facial layer thickness varies periodically with coordinates x and y and is expressed as

$$h_1(x, y) = c_{1m} + b_{1r} \cos \frac{2k_1 \pi x}{a} \cos \frac{2k_2 \pi y}{b} \tag{5}$$

where c_{1m} is the non-periodic part of the thickness, b_{1r} is the wave amplitude of the periodic part of the thickness, and k_1 and k_2 are wave numbers of the periodic part of the thickness.

The facial layer thickness is periodic and needs to be optimized based on a passive spatial periodicity strategy.

2.1. Displacements and Stresses of Sandwich Plate

Under the assumptions, transverse plate displacement relative to support is $w = w(x,y,t)$. Horizontal displacements of upper and lower facial layers in the coordinate x and y directions are expressed as [15]

$$u_1(x,y,z_1,t) = u_{10}(x,y,t) - z_1 \frac{\partial w}{\partial x} \tag{6}$$

$$v_1(x,y,z_1,t) = v_{10}(x,y,t) - z_1 \frac{\partial w}{\partial y} \tag{7}$$

$$u_3(x,y,z_3,t) = u_{30}(x,y,t) - z_3 \frac{\partial w}{\partial x} \tag{8}$$

$$v_3(x,y,z_3,t) = v_{30}(x,y,t) - z_3 \frac{\partial w}{\partial y} \tag{9}$$

where u_{10}, v_{10}, u_{30} and v_{30} are mid-layer displacements and z_1 and z_3 are local transverse coordinates of the two facial layers. With the use of the displacements on the sandwich plate interfaces, shear strains of the core layer obtained are

$$\gamma_{2xz} = \frac{h_a}{h_2} \frac{\partial w}{\partial x} + \frac{u_{10} - u_{30}}{h_2} \tag{10}$$

$$\gamma_{2yz} = \frac{h_a}{h_2} \frac{\partial w}{\partial y} + \frac{v_{10} - v_{30}}{h_2} \tag{11}$$

where $h_a = h_1 + h_2$. Substituting Equations (10) and (11) into Equations (1) and (2) yields the shear stresses of the core layer

$$\tau_{2xz} = G_{2a}\left(\frac{h_a}{h_2} \frac{\partial w}{\partial x} + \frac{u_{10} - u_{30}}{h_2}\right) + G_{2c}\left[\frac{h_a}{h_2} \frac{\partial^2 w}{\partial x \partial t} + \frac{1}{h_2}\left(\frac{\partial u_{10}}{\partial t} - \frac{\partial u_{30}}{\partial t}\right)\right] \tag{12}$$

$$\tau_{2yz} = G_{2a}\left(\frac{h_a}{h_2} \frac{\partial w}{\partial y} + \frac{v_{10} - v_{30}}{h_2}\right) + G_{2c}\left[\frac{h_a}{h_2} \frac{\partial^2 w}{\partial y \partial t} + \frac{1}{h_2}\left(\frac{\partial v_{10}}{\partial t} - \frac{\partial v_{30}}{\partial t}\right)\right] \tag{13}$$

Horizontal normal strains and shear strains of the facial layers are obtained by using geometrical relations with Equations (6)–(9). The corresponding normal stresses and shear stresses (on cross-sections (x,z) and (y,z)) are respectively

$$\sigma_{1x} = \frac{E_1}{1 - \mu^2}\left[\left(\frac{\partial u_{10}}{\partial x} - z_1 \frac{\partial^2 w}{\partial x^2}\right) + \mu\left(\frac{\partial v_{10}}{\partial y} - z_1 \frac{\partial^2 w}{\partial y^2}\right)\right] \tag{14}$$

$$\sigma_{1y} = \frac{E_1}{1 - \mu^2}\left[\left(\frac{\partial v_{10}}{\partial y} - z_1 \frac{\partial^2 w}{\partial y^2}\right) + \mu\left(\frac{\partial u_{10}}{\partial x} - z_1 \frac{\partial^2 w}{\partial x^2}\right)\right] \tag{15}$$

$$\tau_{1xy} = \frac{E_1}{2(1 + \mu)}\left(\frac{\partial u_{10}}{\partial y} + \frac{\partial v_{10}}{\partial x} - 2z_1 \frac{\partial^2 w}{\partial x \partial y}\right) \tag{16}$$

$$\sigma_{3x} = \frac{E_1}{1 - \mu^2}\left[\left(\frac{\partial u_{30}}{\partial x} - z_3 \frac{\partial^2 w}{\partial x^2}\right) + \mu\left(\frac{\partial v_{30}}{\partial y} - z_3 \frac{\partial^2 w}{\partial y^2}\right)\right] \tag{17}$$

$$\sigma_{3y} = \frac{E_1}{1 - \mu^2}\left[\left(\frac{\partial v_{30}}{\partial y} - z_3 \frac{\partial^2 w}{\partial y^2}\right) + \mu\left(\frac{\partial u_{30}}{\partial x} - z_3 \frac{\partial^2 w}{\partial x^2}\right)\right] \tag{18}$$

$$\tau_{3xy} = \frac{E_1}{2(1 + \mu)}\left(\frac{\partial u_{30}}{\partial y} + \frac{\partial v_{30}}{\partial x} - 2z_3 \frac{\partial^2 w}{\partial x \partial y}\right) \tag{19}$$

Based on equilibrium conditions in the coordinate x and y directions with Equations (14)–(19), the other shear stresses of the facial layers obtained are

$$
\begin{aligned}
\tau_{1xz} = & -\frac{E_1}{1-\mu^2}\{\frac{\partial^2 u_{10}}{\partial x^2}(z_1 - \frac{h_1}{2}) + \frac{\partial^3 w}{\partial x^3}(\frac{h_1^2}{8} - \frac{z_1^2}{2}) \\
& +\mu[\frac{\partial^2 v_{10}}{\partial y \partial x}(z_1 - \frac{h_1}{2}) + \frac{\partial^3 w}{\partial y^2 \partial x}(\frac{h_1^2}{8} - \frac{z_1^2}{2})]\} \\
& -\frac{E_1}{2(1+\mu)}[\frac{\partial^2 u_{10}}{\partial y^2}(z_1 - \frac{h_1}{2}) + \frac{\partial^2 v_{10}}{\partial y \partial x}(z_1 - \frac{h_1}{2}) + \frac{\partial^3 w}{\partial y^2 \partial x}(\frac{h_1^2}{4} - z_1^2)]
\end{aligned}
\tag{20}
$$

$$
\begin{aligned}
\tau_{1yz} = & -\frac{E_1}{1-\mu^2}\{\frac{\partial^2 v_{10}}{\partial y^2}(z_1 - \frac{h_1}{2}) + \frac{\partial^3 w}{\partial y^3}(\frac{h_1^2}{8} - \frac{z_1^2}{2}) \\
& +\mu[\frac{\partial^2 u_{10}}{\partial y \partial x}(z_1 - \frac{h_1}{2}) + \frac{\partial^3 w}{\partial x^2 \partial y}(\frac{h_1^2}{8} - \frac{z_1^2}{2})]\} \\
& -\frac{E_1}{2(1+\mu)}[\frac{\partial^2 v_{10}}{\partial x^2}(z_1 - \frac{h_1}{2}) + \frac{\partial^2 u_{10}}{\partial y \partial x}(z_1 - \frac{h_1}{2}) + \frac{\partial^3 w}{\partial x^2 \partial y}(\frac{h_1^2}{4} - z_1^2)]
\end{aligned}
\tag{21}
$$

$$
\begin{aligned}
\tau_{3xz} = & -\frac{E_1}{1-\mu^2}\{\frac{\partial^2 u_{30}}{\partial x^2}(z_3 + \frac{h_1}{2}) + \frac{\partial^3 w}{\partial x^3}(\frac{h_1^2}{8} - \frac{z_3^2}{2}) \\
& +\mu[\frac{\partial^2 v_{30}}{\partial y \partial x}(z_3 + \frac{h_1}{2}) + \frac{\partial^3 w}{\partial y^2 \partial x}(\frac{h_1^2}{8} - \frac{z_3^2}{2})]\} \\
& -\frac{E_1}{2(1+\mu)}[\frac{\partial^2 u_{30}}{\partial y^2}(z_3 + \frac{h_1}{2}) + \frac{\partial^2 v_{30}}{\partial y \partial x}(z_3 + \frac{h_1}{2}) + \frac{\partial^3 w}{\partial y^2 \partial x}(\frac{h_1^2}{4} - z_3^2)]
\end{aligned}
\tag{22}
$$

$$
\begin{aligned}
\tau_{3yz} = & -\frac{E_1}{1-\mu^2}\{\frac{\partial^2 v_{30}}{\partial y^2}(z_3 + \frac{h_1}{2}) + \frac{\partial^3 w}{\partial y^3}(\frac{h_1^2}{8} - \frac{z_3^2}{2}) \\
& +\mu[\frac{\partial^2 u_{30}}{\partial y \partial x}(z_3 + \frac{h_1}{2}) + \frac{\partial^3 w}{\partial x^2 \partial y}(\frac{h_1^2}{8} - \frac{z_3^2}{2})]\} \\
& -\frac{E_1}{2(1+\mu)}[\frac{\partial^2 v_{30}}{\partial x^2}(z_3 + \frac{h_1}{2}) + \frac{\partial^2 u_{30}}{\partial y \partial x}(z_3 + \frac{h_1}{2}) + \frac{\partial^3 w}{\partial x^2 \partial y}(\frac{h_1^2}{4} - z_3^2)]
\end{aligned}
\tag{23}
$$

2.2. Dynamic Equations of Sandwich Plate Coupled with Supported Masses

With the use of continuity conditions of the shear stresses on the sandwich plate interfaces, the differential equations for the horizontal displacements are obtained. They are

$$
\begin{aligned}
& \frac{E_1 h_1}{1-\mu^2}(\frac{\partial^2 u}{\partial x^2} + \mu\frac{\partial^2 v}{\partial y \partial x}) + \frac{E_1 h_1}{2(1+\mu)}(\frac{\partial^2 u}{\partial y^2} + \frac{\partial^2 v}{\partial y \partial x}) \\
& = G_{2a}(\frac{h_a}{h_2}\frac{\partial w}{\partial x} + \frac{2}{h_2}u) + G_{2c}(\frac{h_a}{h_2}\frac{\partial^2 w}{\partial x \partial t} + \frac{2}{h_2}\frac{\partial u}{\partial t})
\end{aligned}
\tag{24}
$$

$$
\begin{aligned}
& \frac{E_1 h_1}{1-\mu^2}(\frac{\partial^2 v}{\partial y^2} + \mu\frac{\partial^2 u}{\partial y \partial x}) + \frac{E_1 h_1}{2(1+\mu)}(\frac{\partial^2 v}{\partial x^2} + \frac{\partial^2 u}{\partial y \partial x}) \\
& = G_{2a}(\frac{h_a}{h_2}\frac{\partial w}{\partial y} + \frac{2}{h_2}v) + G_{2c}(\frac{h_a}{h_2}\frac{\partial^2 w}{\partial y \partial t} + \frac{2}{h_2}\frac{\partial v}{\partial t})
\end{aligned}
\tag{25}
$$

where $u = u_{10} = -u_{30}$ and $v = v_{10} = -v_{30}$, which is due to zero longitudinal force and then anti-symmetric motions of the upper and lower facial layers.

The distributed masses are transversely supported on the plate by springs and dampers, and thus the coupling stiffness and damping are taken into account. Then, the masses dynamics are considered, which act on the plate by the spring and damper forces. The dynamic equation of the sandwich plate element coupled with the supported masses in the coordinate z direction is

$$
\begin{aligned}
& \sum_{i=1}^{3} \int_{-h_i/2}^{h_i/2}(\frac{\partial \tau_{ixz}}{\partial x} + \frac{\partial \tau_{iyz}}{\partial y})dz_i - \rho h_t(\frac{\partial^2 w}{\partial t^2} + \frac{d^2 w_0}{dt^2}) \\
& -\sum_{k=1}^{n_a}[c_{mk}(\frac{\partial w_{pk}}{\partial t} - \frac{d w_{mk}}{dt}) + k_{mk}(w_{pk} - w_{mk})]\delta(x - x_k)\delta(y - y_k) = 0
\end{aligned}
\tag{26}
$$

where $w_{pk} = w(x_k, y_k, t)$ is transverse displacement of the plate on the coupling point (x_k, y_k) relative to the support and (x_k, y_k) are coordinates of the kth mass, $w_{mk}(t)$ is vertical displacement of the kth mass relative to the support, $\delta(\cdot)$ is the Dirac delta function, n_a is total number of masses, $\rho h_t = 2\rho h_1 + \rho h_2$ and $h_t = 2h_1 + h_2$. Substituting Equations (12),

(13) and (20)–(23) into Equation (26) leads to the differential equation for the transverse displacement of the sandwich plate with masses

$$
\begin{aligned}
&\rho h_t \frac{\partial^2 w}{\partial t^2} + D_1 \frac{\partial}{\partial x}\left[h_1^3\left(\frac{\partial^3 w}{\partial x^3} + \frac{\partial^3 w}{\partial y^2 \partial x}\right)\right] + D_1 \frac{\partial}{\partial y}\left[h_1^3\left(\frac{\partial^3 w}{\partial y^3} + \frac{\partial^3 w}{\partial x^2 \partial y}\right)\right] \\
&\quad - \frac{\partial}{\partial x}\left[G_{2a}\frac{h_a^2}{h_2}\left(\frac{\partial w}{\partial x} + \frac{2u}{h_a}\right) + G_{2c}\frac{h_a^2}{h_2}\left(\frac{\partial^2 w}{\partial x \partial t} + \frac{2}{h_a}\frac{\partial u}{\partial t}\right)\right] \\
&\quad - \frac{\partial}{\partial y}\left[G_{2a}\frac{h_a^2}{h_2}\left(\frac{\partial w}{\partial y} + \frac{2v}{h_a}\right) + G_{2c}\frac{h_a^2}{h_2}\left(\frac{\partial^2 w}{\partial y \partial t} + \frac{2}{h_a}\frac{\partial v}{\partial t}\right)\right] \\
&\quad + \sum_{k=1}^{n_a}\left[c_{mk}\left(\frac{\partial w_{pk}}{\partial t} - \frac{\mathrm{d}w_{mk}}{\mathrm{d}t}\right) + k_{mk}(w_{pk} - w_{mk})\right]\delta(x - x_k)\delta(y - y_k) \\
&= -\rho h_t \frac{\mathrm{d}^2 w_0}{\mathrm{d}t^2}
\end{aligned}
\tag{27}
$$

where $D_1 = E_1/6(1 - \mu^2)$. The dynamic equation for the kth mass ($k = 1, 2, \ldots, n_a$) with coupling stiffness and damping is

$$
m_{mk}\frac{\mathrm{d}^2 w_{mk}}{\mathrm{d}t^2} + c_{mk}\left(\frac{\mathrm{d}w_{mk}}{\mathrm{d}t} - \frac{\partial w_{pk}}{\partial t}\right) + k_{mk}(w_{mk} - w_{pk}) = -m_{mk}\frac{\mathrm{d}^2 w_0}{\mathrm{d}t^2}
\tag{28}
$$

Equations (24), (25), (27) and (28) represent a dynamic system that consists of partial and ordinary differential coupling equations with space-varying parameters and random excitation. The partial and ordinary differential coupling system is derived from the sandwich plate coupled with distributed supported masses and describes its coupling transverse and longitudinal motions. Coefficients h_1, G_{2a} and G_{2c} in the plate equations are periodic functions of coordinates x and y, and the plate is coupled with the masses by stiffness and damping. Constraint conditions can be determined based on various given displacements and forces of sandwich plates. The constraint conditions for the boundary simply supported rectangular plate (Figure 1) are [15]

$$
\begin{aligned}
&w\left(\pm\tfrac{a}{2}, y, t\right) = 0, \ w\left(x, \pm\tfrac{b}{2}, t\right) = 0, \ \frac{\partial^2 w(\pm a/2, y, t)}{\partial x^2} = 0, \\
&\frac{\partial^2 w(x, \pm b/2, t)}{\partial y^2} = 0 \\
&\frac{\partial u(\pm a/2, y, t)}{\partial x} + \mu\frac{\partial v(\pm a/2, y, t)}{\partial y} = 0, \ \frac{\partial v(x, \pm b/2, t)}{\partial y} + \mu\frac{\partial u(x, \pm b/2, t)}{\partial x} = 0
\end{aligned}
\tag{29}
$$

By introducing the non-dimensional (ND) coordinates and displacements

$$
\begin{aligned}
&\bar{x} = \tfrac{x}{a}, \ \bar{y} = \tfrac{y}{b}, \ \bar{x}_k = \tfrac{x_k}{a}, \ \bar{y}_k = \tfrac{y_k}{b}, \ \bar{u} = \tfrac{u}{w_a}, \ \bar{v} = \tfrac{v}{w_a} \\
&\bar{w} = \tfrac{w}{w_a}, \ \bar{w}_0 = \tfrac{w_0}{w_a}, \ \bar{w}_{pk} = \tfrac{w_{pk}}{w_a}, \ \bar{w}_{mk} = \tfrac{w_{mk}}{w_a}
\end{aligned}
\tag{30}
$$

where w_a is the amplitude of support motion w_0, the differential Equations (27), (28), (24) and (25) and the boundary conditions (29) become

$$
\begin{aligned}
&\rho h_t \frac{\partial^2 \bar{w}}{\partial t^2} + D_1 \frac{\partial}{\partial \bar{x}}\left[\frac{h_1^3}{a^4}\left(\frac{\partial^3 \bar{w}}{\partial \bar{x}^3} + \frac{a^2}{b^2}\frac{\partial^3 \bar{w}}{\partial \bar{y}^2 \partial \bar{x}}\right)\right] + D_1 \frac{\partial}{\partial \bar{y}}\left[\frac{h_1^3}{b^4}\left(\frac{\partial^3 \bar{w}}{\partial \bar{y}^3} + \frac{b^2}{a^2}\frac{\partial^3 \bar{w}}{\partial \bar{x}^2 \partial \bar{y}}\right)\right] \\
&\quad - \frac{\partial}{\partial \bar{x}}\left[G_{2a}\frac{h_a^2}{a^2 h_2}\left(\frac{\partial \bar{w}}{\partial \bar{x}} + \frac{2a\bar{u}}{h_a}\right) + G_{2c}\frac{h_a^2}{a^2 h_2}\left(\frac{\partial^2 \bar{w}}{\partial \bar{x} \partial t} + \frac{2a}{h_a}\frac{\partial \bar{u}}{\partial t}\right)\right] \\
&\quad - \frac{\partial}{\partial \bar{y}}\left[G_{2a}\frac{h_a^2}{b^2 h_2}\left(\frac{\partial \bar{w}}{\partial \bar{y}} + \frac{2b\bar{v}}{h_a}\right) + G_{2c}\frac{h_a^2}{b^2 h_2}\left(\frac{\partial^2 \bar{w}}{\partial \bar{y} \partial t} + \frac{2b}{h_a}\frac{\partial \bar{v}}{\partial t}\right)\right] \\
&\quad + \sum_{k=1}^{n_a}\left[c_{0k}\left(\frac{\partial \bar{w}_{pk}}{\partial t} - \frac{\mathrm{d}\bar{w}_{mk}}{\mathrm{d}t}\right) + k_{0k}\left(\bar{w}_{pk} - \bar{w}_{mk}\right)\right]\delta(\bar{x} - \bar{x}_k)\delta(\bar{y} - \bar{y}_k) \\
&= -\rho h_t \frac{\mathrm{d}^2 \bar{w}_0}{\mathrm{d}t^2}
\end{aligned}
\tag{31}
$$

$$
m_{0k}\frac{\mathrm{d}^2 \bar{w}_{mk}}{\mathrm{d}t^2} + c_{0k}\left(\frac{\mathrm{d}\bar{w}_{mk}}{\mathrm{d}t} - \frac{\partial \bar{w}_{pk}}{\partial t}\right) + k_{0k}(\bar{w}_{mk} - \bar{w}_{pk}) = -m_{0k}\frac{\mathrm{d}^2 \bar{w}_0}{\mathrm{d}t^2}
\tag{32}
$$

$$
\begin{aligned}
&6D_1 h_1\left(\frac{\partial^2 \bar{u}}{a^2 \partial \bar{x}^2} + \frac{1-\mu}{2b^2}\frac{\partial^2 \bar{u}}{\partial \bar{y}^2} + \frac{1+\mu}{2ab}\frac{\partial^2 \bar{v}}{\partial \bar{y} \partial \bar{x}}\right) \\
&= G_{2a}\left(\frac{h_a}{ah_2}\frac{\partial \bar{w}}{\partial \bar{x}} + \frac{2\bar{u}}{h_2}\right) + G_{2c}\left(\frac{h_a}{ah_2}\frac{\partial^2 \bar{w}}{\partial \bar{x} \partial t} + \frac{2}{h_2}\frac{\partial \bar{u}}{\partial t}\right)
\end{aligned}
\tag{33}
$$

$$6D_1h_1\left(\frac{\partial^2\overline{v}}{b^2\partial\overline{y}^2} + \frac{1-\mu}{2a^2}\frac{\partial^2\overline{v}}{\partial\overline{x}^2} + \frac{1+\mu}{2ab}\frac{\partial^2\overline{u}}{\partial\overline{y}\partial\overline{x}}\right)$$
$$= G_{2a}\left(\frac{h_a}{bh_2}\frac{\partial\overline{w}}{\partial\overline{y}} + \frac{2\overline{v}}{h_2}\right) + G_{2c}\left(\frac{h_a}{bh_2}\frac{\partial^2\overline{w}}{\partial\overline{y}\partial t} + \frac{2}{h_2}\frac{\partial\overline{v}}{\partial t}\right) \tag{34}$$

$$\overline{w}\left(\pm\tfrac{1}{2},\overline{y},t\right) = 0,\ \overline{w}\left(\overline{x},\pm\tfrac{1}{2},t\right) = 0,$$
$$\frac{\partial^2\overline{w}(\pm 1/2,\overline{y},t)}{\partial\overline{x}^2} = 0,\ \frac{\partial^2\overline{w}(\overline{x},\pm 1/2,t)}{\partial\overline{y}^2} = 0 \tag{35}$$
$$\frac{\partial\overline{u}(\pm 1/2,\overline{y},t)}{\partial\overline{x}} + \mu\frac{\partial\overline{v}(\pm 1/2,\overline{y},t)}{\partial\overline{y}} = 0,\ \frac{\partial\overline{v}(\overline{x},\pm 1/2,t)}{\partial\overline{y}} + \mu\frac{\partial\overline{u}(\overline{x},\pm 1/2,t)}{\partial\overline{x}} = 0$$

3. Stochastic Response Analysis of Partial and Ordinary Differential Coupling System

Vibration mode functions of the plate are determined based on boundary constraint conditions, and then the plate displacements can be expanded by using the modes. For the simply supported rectangular plate with Equation (35), the non-dimensional (ND) vibration displacements of the sandwich plate are expanded as

$$\overline{u} = \sum_{i=1}^{N_1}\sum_{j=1}^{N_2} r_{ij}(t)\sin[(2i-1)\pi\overline{x}]\cos[(2j-1)\pi\overline{y}] \tag{36}$$

$$\overline{v} = \sum_{i=1}^{N_1}\sum_{j=1}^{N_2} s_{ij}(t)\cos[(2i-1)\pi\overline{x}]\sin[(2j-1)\pi\overline{y}] \tag{37}$$

$$\overline{w} = \sum_{i=1}^{N_1}\sum_{j=1}^{N_2} q_{ij}(t)\cos[(2i-1)\pi\overline{x}]\cos[(2j-1)\pi\overline{y}] \tag{38}$$

where $r_{ij}(t)$, $s_{ij}(t)$ and $q_{ij}(t)$ are functions of time representing generalized displacements and N_1 and N_2 are integers representing expansion term numbers. The masses are distributed on the plate symmetrically about coordinates x and y. According to the Galerkin method, substituting Equations (36)–(38) into Equations (31), (33) and (34); multiplying the equations by $\cos[(2i-1)\pi\overline{x}]\cos[(2j-1)\pi\overline{y}]$, $\sin[(2i-1)\pi\overline{x}]\cos[(2j-1)\pi\overline{y}]$ and $\cos[(2i-1)\pi\overline{x}]\sin[(2j-1)\pi\overline{y}]$, respectively; and integrating them with respect to $\overline{x}$ and $\overline{y}$ yield ordinary differential equations for q_{ij}, r_{ij} and s_{ij}. It is noted that the horizontal velocity terms are relatively small. By eliminating r_{ij} and s_{ij}, the ordinary differential equations for generalized transverse displacement q_{ij} which describe the multi-mode coupling vibration of the sandwich plate can be obtained. The equations for q_{ij} combined with equation (32) for masses are rewritten in the matrix form

$$\mathbf{M}\frac{d^2\mathbf{Q}}{dt^2} + \mathbf{C}\frac{d\mathbf{Q}}{dt} + \mathbf{K}\mathbf{Q} = \mathbf{F}(t) \tag{39}$$

where generalized excitation vector $\mathbf{F}(t) = -\mathbf{F}_C d^2\overline{w}_0/dt^2$, generalized displacement vector $\mathbf{Q}$, mass matrix $\mathbf{M}$, damping matrix $\mathbf{C}$, stiffness matrix $\mathbf{K}$ and vector $\mathbf{F}_C$ are given in Appendix A, in which elements in the matrices and vectors are determined by the spatial integrals of coefficients in Equations (31)–(34).

Equation (39) is a unified ordinary differential coupling equation and represents a stochastically excited multi-degree-of-freedom system derived from the visco-elastomer sandwich plate coupled with supported masses under support excitations. The generalized mass, damping and stiffness of the system depend on periodic distribution parameters such as k_1, k_2, k_a, k_b, b_{1r}, b_{a1} and b_{c1} and coupling stiffness k_{0k} and coupling damping c_{0k}. The vibration response of the system with a sandwich plate and supported masses can be estimated by using power spectral density functions. The frequency response function and response spectral density matrices of the system (39) are obtained and expressed as

$$\mathbf{H}(\omega) = \left(\mathbf{K} + j\omega\mathbf{C} - \omega^2\mathbf{M}\right)^{-1} \tag{40}$$

$$\mathbf{S_Q}(\omega) = \mathbf{H}(\omega)\mathbf{F}_C\mathbf{F}_C^{\mathrm{T}}\mathbf{H}^{*\mathrm{T}}(\omega)S_{\ddot{\overline{w}}_0} \tag{41}$$

where $\mathrm{j} = \sqrt{-1}$, ω is vibration frequency, superscript * denotes complex conjugate and $S_{\ddot{\overline{w}}_0}(\omega)$ is the power spectral density of support excitation. By using Equations (41) and (38), the spectral density function of the ND transverse displacement of the plate is expressed as

$$S_{\overline{w}}(\omega, \overline{x}, \overline{y}) = \mathbf{\Phi}^{\mathrm{T}}(\overline{x}, \overline{y})\mathbf{S_Q}(\omega)\mathbf{\Phi}(\overline{x}, \overline{y}) \tag{42}$$

where

$$\mathbf{\Phi}(\overline{x}, \overline{y}) = [\mathbf{\Phi}_1^{\mathrm{T}}\ \mathbf{\Phi}_2^{\mathrm{T}}\ ...\ \mathbf{\Phi}_{N_2}^{\mathrm{T}}\ \ 0]^{\mathrm{T}},\ \mathbf{\Phi}_j = \begin{bmatrix} \varphi_{1j} & \varphi_{2j} & ... & \varphi_{N_1j} \end{bmatrix}^{\mathrm{T}}$$
$$\phi_{ij} = \cos[(2i-1)\pi\overline{x}]\cos[(2j-1)\pi\overline{y}] \tag{43}$$

The spectral density function of the ND transverse displacement of the masses is accordingly

$$S_{mk_1k_2}(\omega) = [\mathbf{S_Q}(\omega)]_{N_1N_2+k_1, N_1N_2+k_2} \tag{44}$$

The auto-power spectral density of the displacement of the kth mass is

$$S_{mk}(\omega) = [\mathbf{S_Q}(\omega)]_{N_1N_2+k, N_1N_2+k} \tag{45}$$

Response statistics of the sandwich plate and supported masses under random excitations are estimated by using the spectral density functions. For example, the mean square displacement responses of the plate and mass are, respectively,

$$E[\overline{w}^2(\overline{x}, \overline{y})] = \int_{-\infty}^{+\infty} S_{\overline{w}}(\omega, \overline{x}, \overline{y})\mathrm{d}\omega \tag{46}$$

$$E[\overline{w}_{mk}^2] = \int_{-\infty}^{+\infty} S_{mk}(\omega)\mathrm{d}\omega \tag{47}$$

where $E[\cdot]$ is the expectation operation of a stochastic process and is equal to the average over the time domain for an ergodic process. Using Equations (42) and (45), response characteristics of the sandwich plate with supported masses adjusted by periodic geometrical and physical parameters are explored.

4. Numerical Results and Discussion

To show the frequency response characteristics and response reduction performance, consider a visco-elastomer sandwich plate coupled with supported masses under support excitation. Its facial layer thickness is spatially periodic and its core layer modulus is also spatially periodic and can be adjusted by external control action. The coupling plate and mass system has the following parameter values: $a = 4$ m, $b = 2$ m, $\rho_1 = 3000$ kg/m^3, $\rho_2 = 1200$ kg/m^3, $E_1 = 10$ GPa, $\mu = 0.3$, $e_{a1} = 4$ MPa, $b_{a1} = \beta e_{a1}$, $e_{c1} = 0.006$ MPa·s, $b_{c1} = \beta e_{c1}$, $c_{1m} = 0.05$ m, $b_{1r} = \alpha c_{1m}$, $h_2 = 0.2$ m, $\alpha = 0.3$, $\beta = 0.5$, $w_a = 1$, $n_a = 1$, $x_1 = y_1 = 0$, $m_{01} = 240$ kg/m^2, $k_{01} = 1.8 \times 10^3$ kN/m^3 and $c_{01} = 0.8$ kN·s/m^3 unless otherwise specified. The support excitation is a zero-mean random process with the Kanai–Tajimi power spectral density

$$S_{\ddot{\overline{w}}_0}(\omega) = \frac{1 + 4\zeta_g^2(\omega/\omega_g)^2}{\left[1 - (\omega/\omega_g)^2\right]^2 + 4\zeta_g^2(\omega/\omega_g)^2}S_0 \tag{48}$$

where non-dimensional (ND) excitation intensity $S_0 = 1$, $\omega_g = 23$ rad/s and $\zeta_g = 0.3$ unless otherwise specified. The stochastic responses of the sandwich plate with supported masses are calculated by using Equations (40)–(47) in MATLAB. Numbers N_1 and N_2 in Equation (38) are determined by the convergence of displacement responses ($N_1 = N_2 = 18$ used). The logarithmic ND (LND) displacement response spectra of the sandwich plate at the midpoint under unit periodic support excitation have been verified by the finite element method as shown in Figure 2. Numerical results on stochastic responses and response spectral densities of the plate and masses are shown in Figures 3–15.
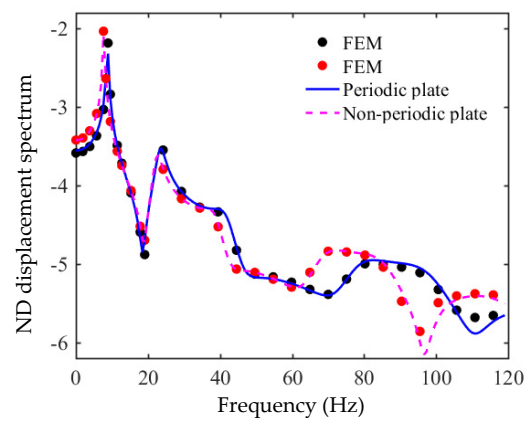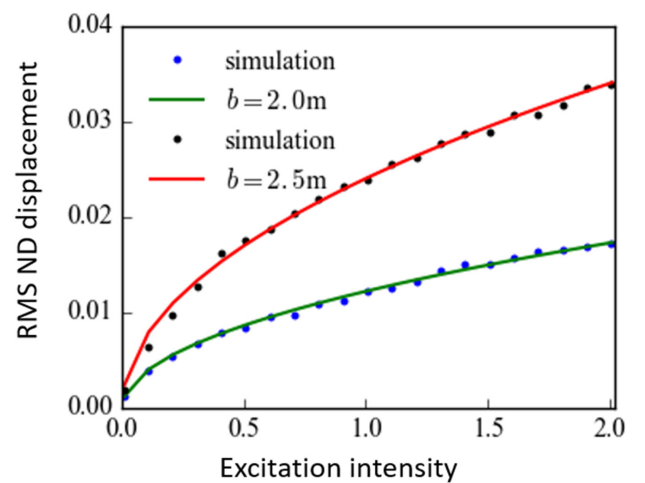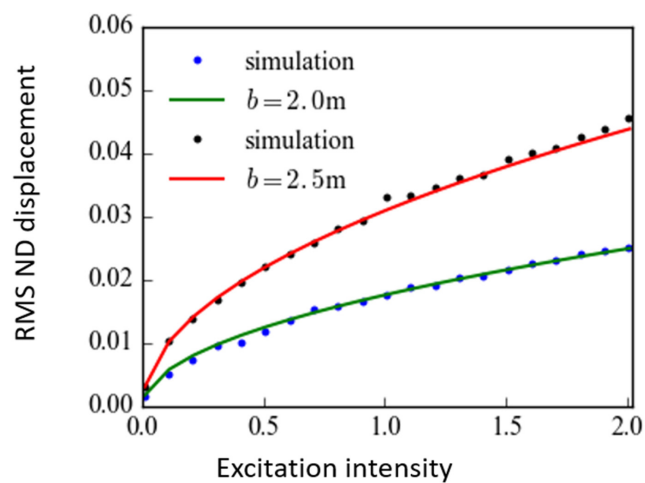
Figure 2. LND displacement spectra of non-periodic and periodic sandwich plates under periodic excitation (FEM: finite element method).
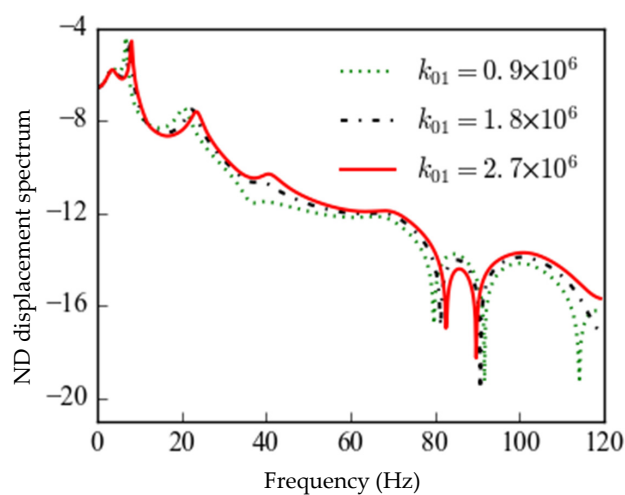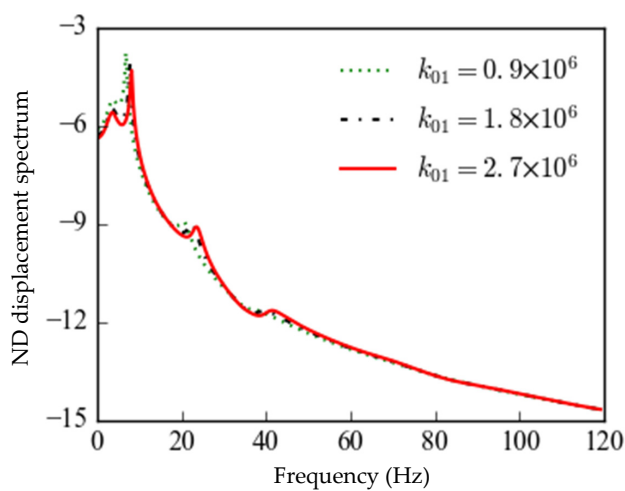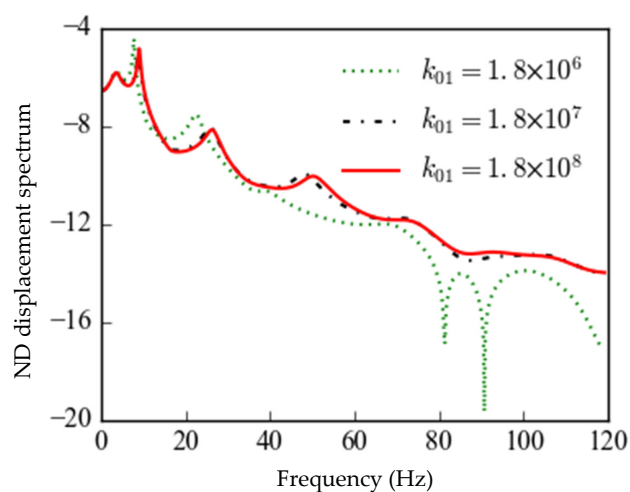

(**a**) Plate

(**b**) Mass

Figure 3. RMS ND displacement responses of sandwich plate with mass versus ND excitation intensity (S_0).
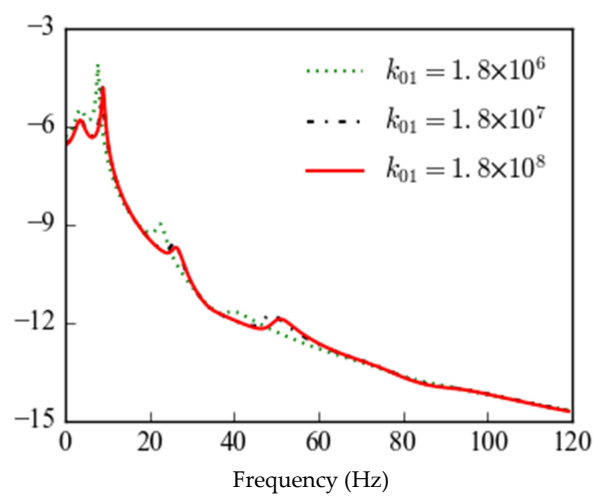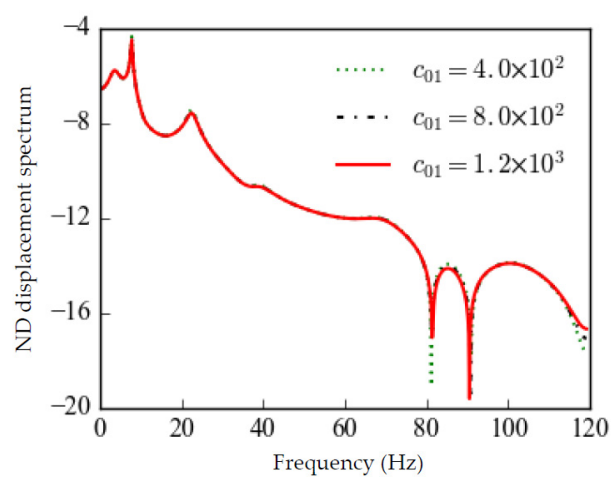
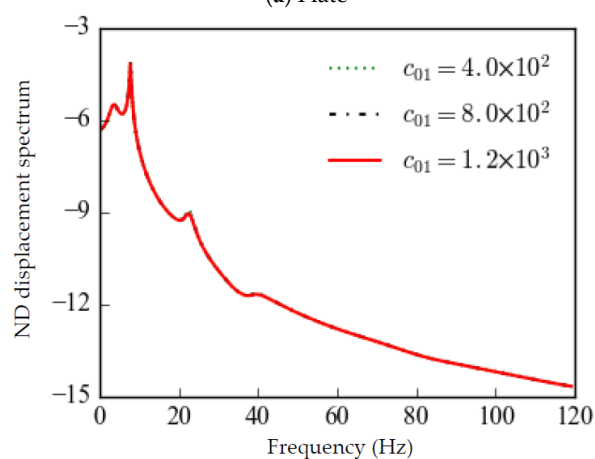(**a**) Plate

(**b**) Mass

(**c**) Plate

Figure 4. *Cont.*

(**d**) Mass

Figure 4. LND displacement spectra of plate with mass for different stiffnesses (k_{01}).

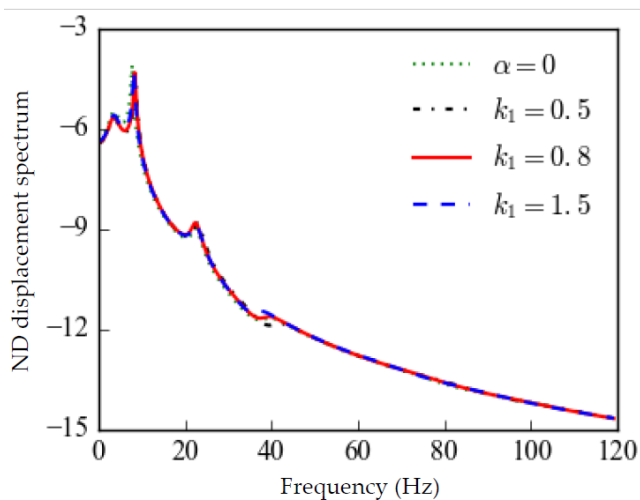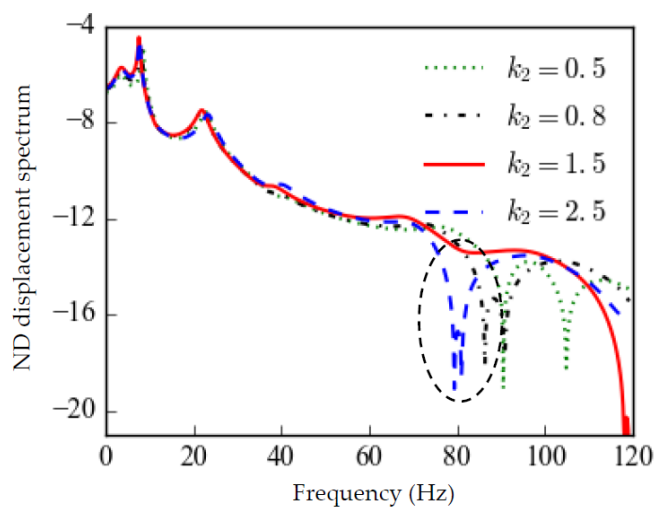(**a**) Plate

(**b**) Mass

Figure 5. LND displacement spectra of plate with mass for different dampings (c_{01}).
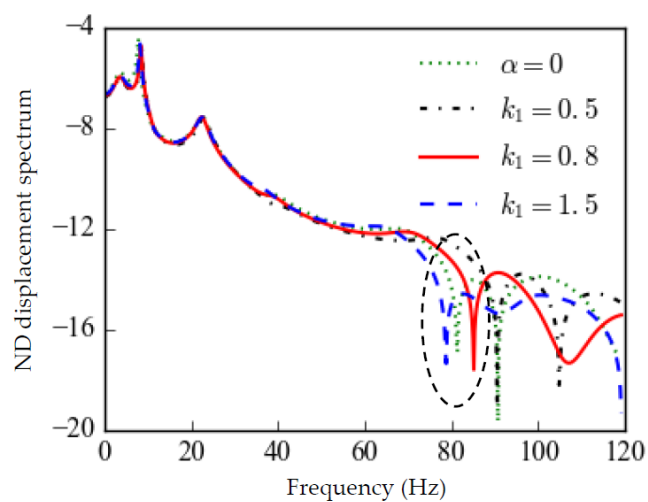
(**a**) Plate

(**b**) Mass

Figure 6. LND displacement spectra of plate with mass for different thickness wave numbers (k_1).

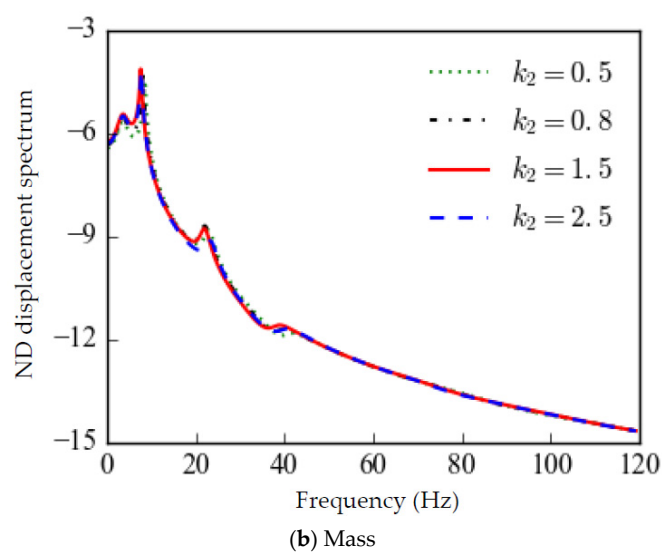(**a**) Plate

Figure 7. *Cont.*

(**b**) Mass

Figure 7. LND displacement spectra of plate with mass for different thickness wave numbers (k_2).
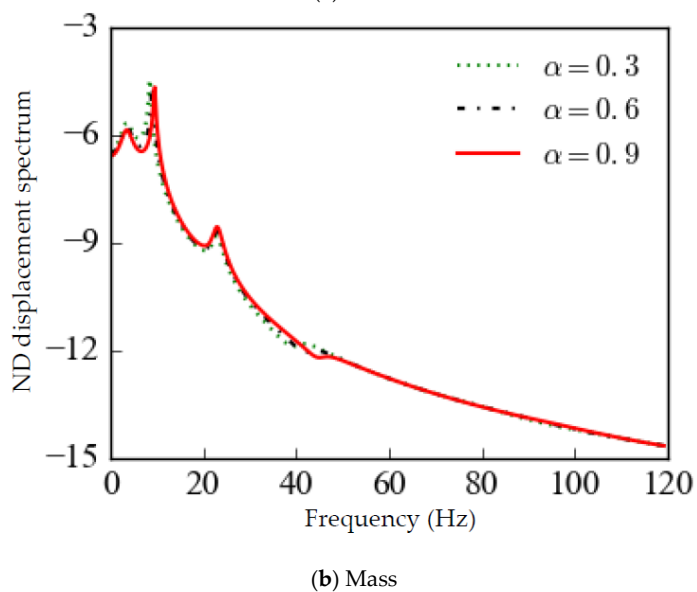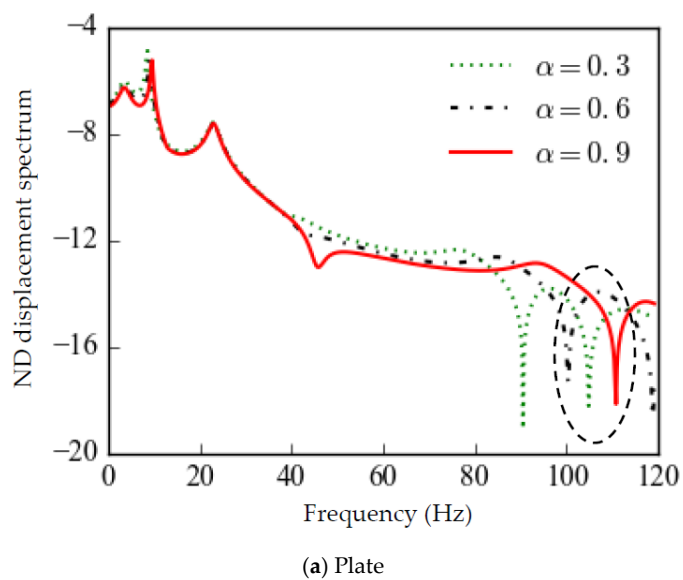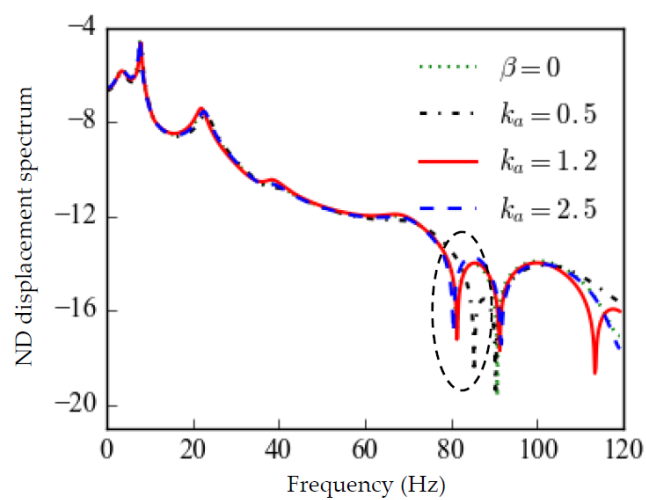

(**a**) Plate
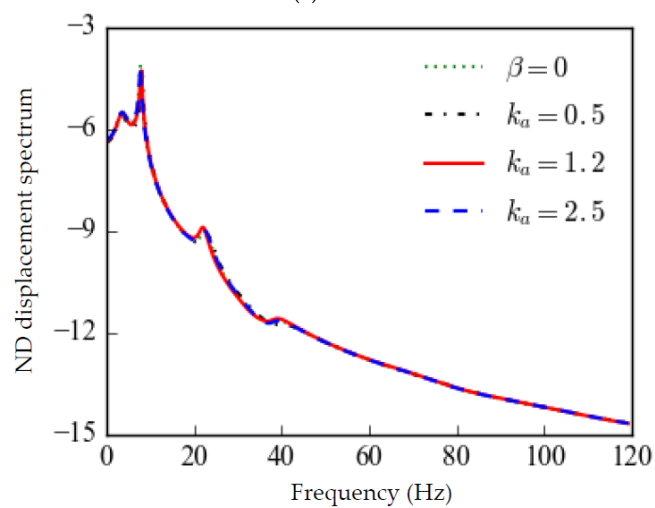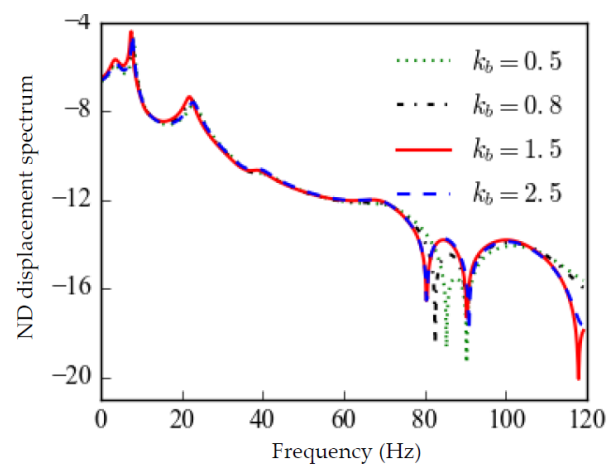

(**b**) Mass

Figure 8. LND displacement spectra of plate with mass for different values of parameter α.

(**a**) Plate

(**b**) Mass

Figure 9. LND displacement spectra of plate with mass for different modulus wave numbers (k_a).

(**a**) Plate

Figure 10. *Cont.*

(**b**) Mass

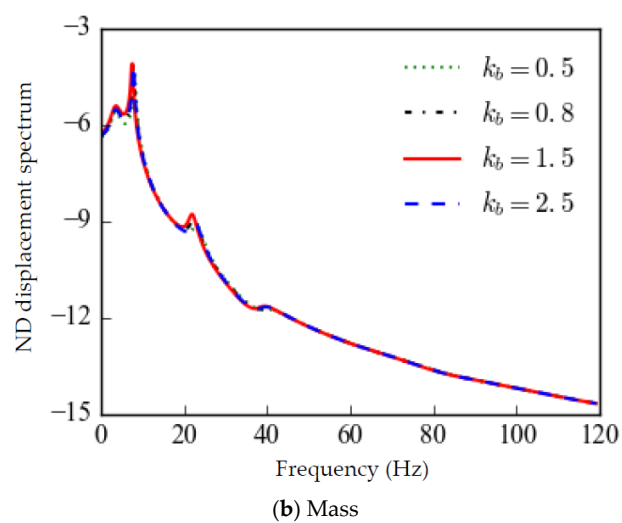**Figure 10.** LND displacement spectra of plate with mass for different modulus wave numbers (k_b).
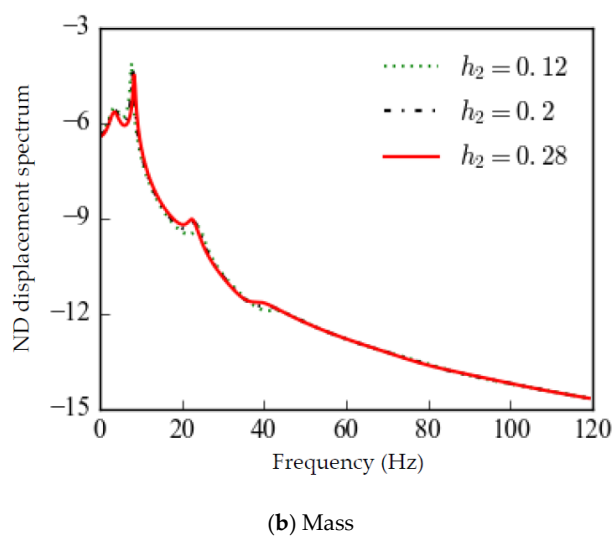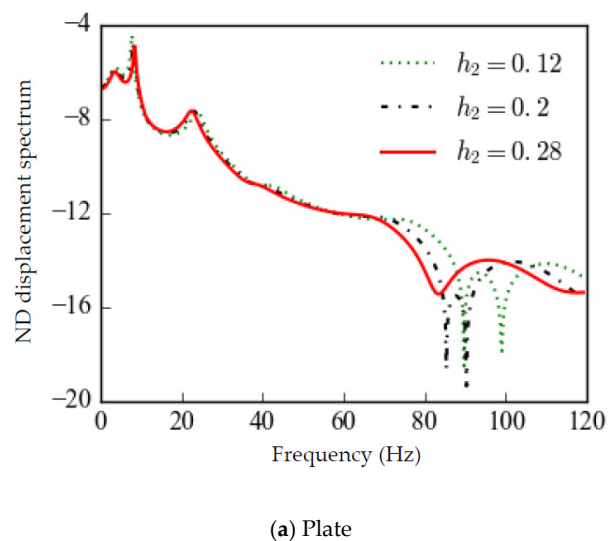
(**a**) Plate

(**b**) Mass

Figure 11. LND displacement spectra of plate with mass for different core layer thicknesses (h_2).
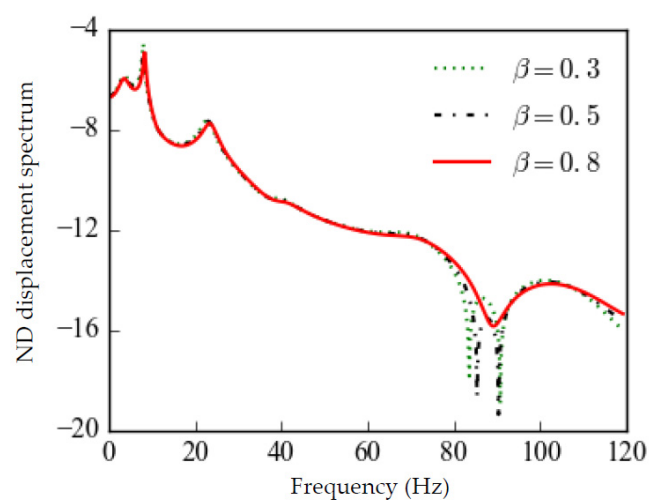
(**a**) Plate
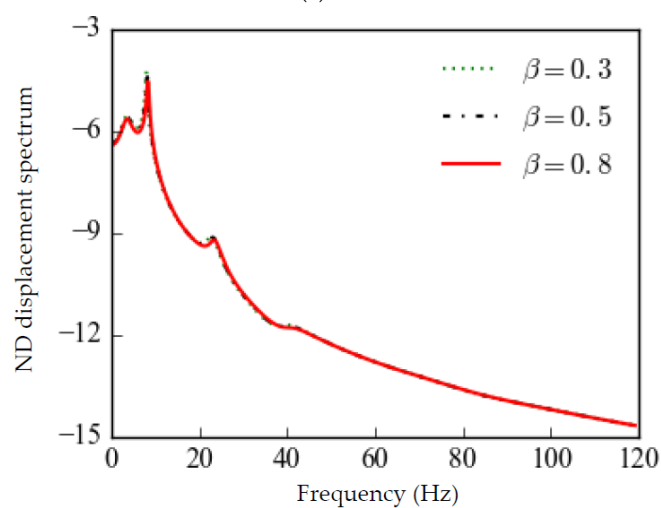
(**b**) Mass

Figure 12. LND displacement spectra of plate with mass for different values of parameter β.
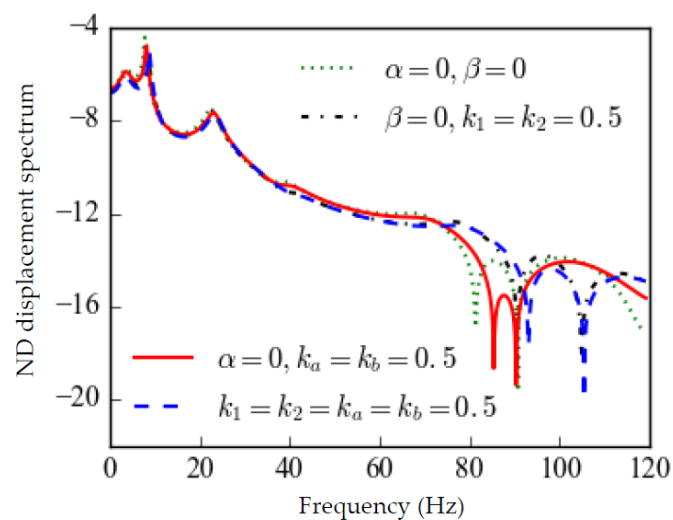
(**a**) Plate

Figure 13. *Cont.*

(**b**) Mass

Figure 13. LND displacement spectra of plate with mass for different wave amplitudes and wave numbers.

(**a**) Plate

(**b**) Mass

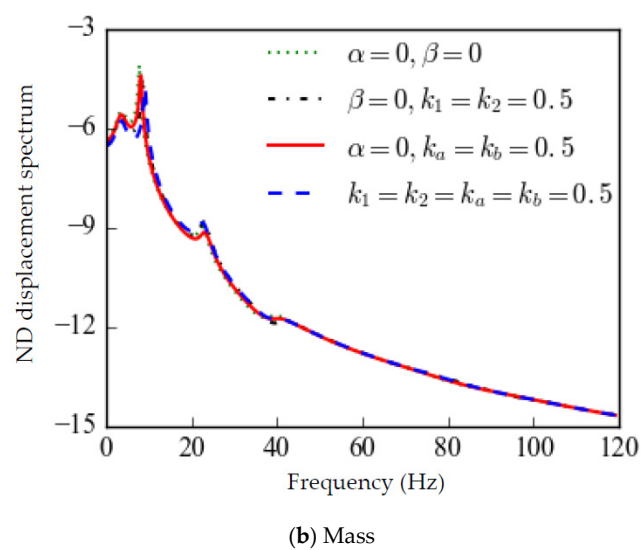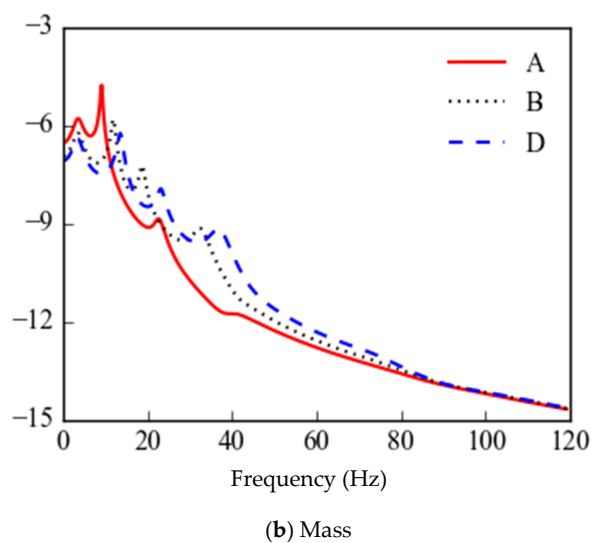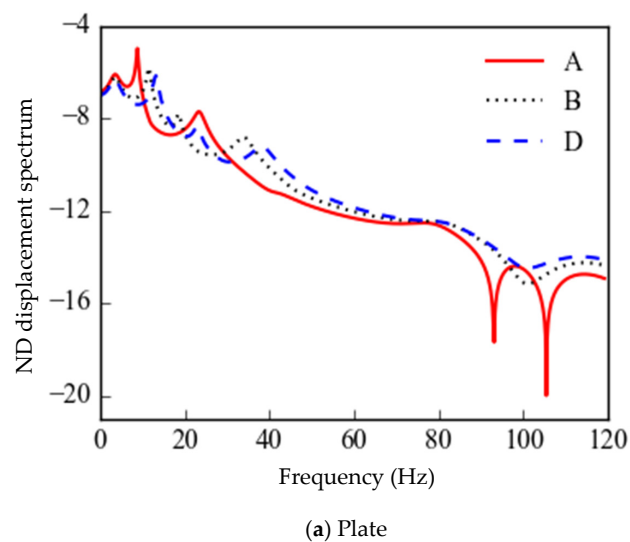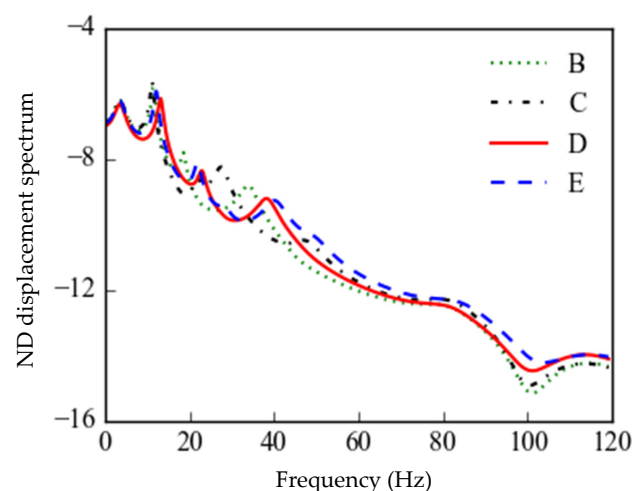**Figure 14.** LND displacement spectra of plate with masses for cases A, B and D.

(**a**) Plate
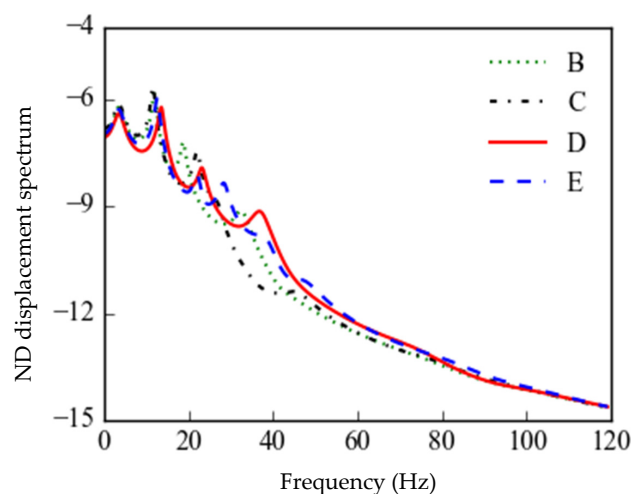
Figure 15. LND displacement spectra of plate with masses for cases B, C, D and E.

Figure 3a,b shows that the root-mean-square (RMS) ND displacement ($\overline{w}$) responses of the sandwich plate (b = 2 m, 2.5 m) at the midpoint and supported mass ($x_1 = y_1 = 0$) with uniform distribution parameters ($b_{1r} = 0$, $b_{a1} = 0$, $b_{c1} = 0$) vary with the ND excitation intensity (S_0), respectively. The RMS displacement responses of the plate with mass obtained by numerical simulation verify the results obtained by the proposed analysis method. The numerical simulation procedure includes that samples of the random excitation are generated according to the power spectral density, stochastic responses of Equations (39) and (38) are calculated using the Wilson-theta algorithm, and the response statistics are obtained. It is seen by comparing Figure 3a,b that the RMS displacement response of the mass is larger than that of the plate because the coupling between them is considered and the plate motion can be regarded as excitation to the mass, and this motion is enlarged by coupling stiffness with damping under certain conditions.

4.1. Effects of Coupling Stiffness and Damping on Response

The influence of the coupling stiffness (k_{01}) and damping (c_{01}) between the sandwich plate and supported mass on the displacement response is firstly explored ($\alpha = 0$, $\beta = 0$). Figure 4a,c and Figure 4b,d show the LND displacement spectra of the plate at the midpoint and supported mass ($x_1 = y_1 = 0$) for different coupling stiffnesses (k_{01}), respectively. Several peaks and many valleys seen indicate possible resonance and anti-resonance. As the coupling stiffness decreases from 1.8×10^5 kN/m^3 to 0.9×10^3 kN/m^3, the anti-resonant

response amplitudes, e.g., the third anti-resonant amplitude of the plate, are greatly reduced. The effect of the coupling stiffness on the plate response is larger than the mass response. Thus, the coupling stiffness between the sandwich plate and supported mass has a large effect on the response characteristics, which can change the plate and mass dynamics and needs to be determined suitably. However, the small coupling damping has a slight effect on the displacement response spectra of the sandwich plate with supported mass, as shown in Figure 5a,b.

4.2. Effects of Periodic Facial Layer Thickness on Response

The influence of the periodic distribution of the facial layer thickness (h_1) on the displacement response of the sandwich plate at the midpoint and supported mass ($x_1 = y_1 = 0$) is explored ($\beta = 0$). Figure 6a,b shows the LND displacement spectra of the plate and mass for different thickness wave numbers (k_1) (in coordinate x direction) ($k_2 = 0.5$, $\alpha = 0.3$), respectively. The plate with mass in multi-mode coupling vibration has multiple response resonances and anti-resonances. The wave number k_1 has certain effects on the anti-resonant frequencies and amplitudes; e.g., the fourth anti-resonant frequency of the plate is large and the corresponding amplitude (response valley) is relatively small for the thickness wave number $k_1 \approx 0.8$. The response valley of different anti-resonances has various minimal values for different thickness wave numbers. Thus, the thickness wave number k_1 has a large effect on the response characteristics of the periodic sandwich plate. The response has various adjustable performances in different frequency bands by choosing the wave number.

Figure 7a,b shows the LND displacement spectra of the plate and mass for different thickness wave numbers (k_2) (in coordinate y direction) ($k_1 = 0.5$, $\alpha = 0.3$), respectively. The wave number k_2, similar to k_1, has an obvious effect on the resonant and anti-resonant response amplitudes and frequencies of the plate. The response characteristics can be adjusted in different frequency bands by choosing the wave number, e.g., the fourth anti-resonant amplitude (response valley) of the plate for the thickness wave number $k_2 \approx 2.5$.

Figure 8a,b shows the LND displacement spectra of the plate and mass for different values of the parameter α (ratio of periodic to non-periodic parts of the thickness) ($\beta = 0$, $k_1 = k_2 = 0.5$). It is seen that the anti-resonant frequencies increase with the parameter α and the anti-resonant response amplitudes have minimum values for certain values of the parameter α (e.g., the non-logarithmic spectral amplitude of the fourth anti-resonance of the plate is 8.6×10^{-20}, 5.1×10^{-18} and 7.5×10^{-19} and the fourth anti-resonant frequency is 90.7, 100.7 and 111.1 Hz when the parameter $\alpha = 0.3$, 0.6 and 0.9, respectively; that of the third anti-resonance of the mass is 1.3×10^{-12}, 9.2×10^{-13} and 6.4×10^{-13} and the third anti-resonant frequency is 39.6, 42.4 and 45.2 Hz when the parameter $\alpha = 0.3$, 0.6 and 0.9, respectively). Thus, the ratio of periodic to non-periodic parts of the thickness has an obvious effect on the response characteristics of the sandwich plate and supported mass. The response characteristics, including anti-resonant response amplitudes and frequencies, are greatly adjustable by suitably choosing the ratio or wave amplitude.

4.3. Effects of Periodic Core Layer Modulus on Response

The influence of the periodic distribution of the core layer modulus on the displacement response of the sandwich plate at the midpoint and supported mass ($x_1 = y_1 = 0$) is explored ($\alpha = 0$). Figure 9a,b shows the LND displacement spectra of the plate and mass for different wave numbers of the modulus (k_a) (in coordinate x direction) ($k_b = 0.5$, $\beta = 0.5$), respectively. The wave number k_a has a certain effect on the anti-resonant frequencies and amplitudes; e.g., the fourth anti-resonant frequency of the sandwich plate is large and the corresponding amplitude (response valley) is small relatively for the modulus wave number $k_a \approx 0.5$. The response valley of different anti-resonances has a minimum value for different modulus wave numbers. Figure 10a,b shows the LND displacement spectra of the plate and mass for different modulus wave numbers (k_b) (in coordinate y direction) ($k_a = 0.5$, $\beta = 0.5$), respectively. The wave number k_b, similar to k_a, has an obvious

effect on the resonant and anti-resonant response amplitudes and frequencies of the plate with mass. Thus, the modulus wave numbers k_a and k_b have great effects on the response characteristics of the sandwich plate. The response has various adjustable performances in different frequency bands by choosing the wave numbers.

Figure 11a,b shows the LND displacement spectra of the plate and mass for different core layer thicknesses (h_2) ($k_a = 0.5$, $k_b = 0.5$, $\beta = 0.5$), respectively. The core layer thickness has an obvious effect on the response characteristics including anti-resonant frequencies and amplitudes of the sandwich plate with supported mass. The response has various adjustable performances in different frequency bands by choosing the core layer thickness.

Figure 12a,b shows the LND displacement spectra of the plate and mass for different values of the parameter β (ratio of periodic to non-periodic parts of the modulus) ($\alpha = 0$, $k_a = k_b = 0.5$), respectively. The anti-resonant frequencies increase with the parameter β, and the anti-resonant response amplitude has a minimum value for a certain value of the parameter β. Thus, the ratio of periodic to non-periodic parts of the modulus has a certain effect on the response characteristics of the sandwich plate. The response characteristics, including anti-resonant response amplitudes and frequencies, are adjustable in different frequency bands by choosing the ratio or wave amplitude.

4.4. Effects of Both Periodic Thickness and Modulus on Response

The influence of periodic distribution of both the thickness and modulus on the displacement response of the sandwich plate at the midpoint and supported mass ($x_1 = y_1 = 0$) is further illustrated ($\alpha = 0.3$, $\beta = 0.5$). Figure 13a,b shows the LND displacement spectra of the plate and mass for different wave amplitude ratios (α and β) ($k_1 = k_2 = k_a = k_b = 0.5$) and wave numbers ($k_1$, k_2, k_a and k_b), respectively. The periodic distribution of both the thickness and modulus can reduce certain response peaks and valleys (e.g., the second resonance, fifth anti-resonance) more than the periodic distribution of only the thickness ($\beta = 0$) or only the modulus ($\alpha = 0$). The suitable wave amplitudes and wave numbers of periodic thickness and modulus can further improve the response characteristics of the plate with mass in different frequency bands.

4.5. Effects of Periodically Distributed Masses on Response

The influence of distribution of masses coupled with the plate on the displacement response of the periodic sandwich plate and masses is considered in five cases. Case A is one mass (240 kg/m^2) on the plate with ND coordinates (0, 0). Cases B and C are three equal masses (80 kg/m^2) on the plate with ND coordinates (-0.25, 0), (0, 0) and (0.25, 0) and (0, -0.25), (0, 0) and (0, 0.25), respectively. Cases D and E are five equal masses (48 kg/m^2) on the plate with ND coordinates (-0.25, -0.25), (-0.25, 0.25), (0, 0), (0.25, -0.25) and (0.25, 0.25) and (-0.25, 0), (0, -0.25), (0, 0), (0, 0.25) and (0.25, 0), respectively. The coupling stiffness is $k_{0k} = k_{01}$ and coupling damping is $c_{0k} = c_{01}$ ($k = 2, 3, 4, 5$). Numerical results on the ND displacement response for different mass distributions are shown in Figures 14 and 15 ($k_1 = k_2 = k_a = k_b = 0.5$, $\alpha = 0.3$, $\beta = 0.5$).

Figure 14a,b shows the LND displacement spectra of the plate and mass at the midpoint for cases A, B and D, respectively. The mass decentralization (different numbers, but equal total mass) has a great effect on the response characteristics, including the resonant peaks and anti-resonant valleys and the corresponding frequencies (e.g., the non-logarithmic spectral amplitude of the second resonance of the plate is 1.1×10^{-5}, 1.6×10^{-6} and 7.3×10^{-7} and the second resonant frequency is 9.0, 11.7 and 13.3 Hz for cases A, B and D, respectively; that of the second resonance of the mass is 1.7×10^{-5}, 1.6×10^{-6} and 5.9×10^{-7} and the second resonant frequency is 9.4, 12.1 and 13.7 Hz for cases A, B and D, respectively). The suitable mass decentralization can reduce the peaks and valleys and then improve the response characteristics of the sandwich plate with supported masses. However, the mass decentralization has different effects on response characteristics of the plate and mass in different frequency bands due to the coupling between different masses by the plate.

Figure 15a,b shows the LND displacement spectra of the plate and mass at the midpoint for cases B, C, D and E, respectively. The suitable mass placement (equal numbers, but different placements) can greatly reduce the resonant peaks and anti-resonant valleys and then improve the response characteristics. However, it can be noted that the response in non-anti-resonant frequency bands is larger than that in anti-resonant frequency bands for different mass placements due to anti-resonant frequency variation. In consequence, the response characteristics, including resonant peaks and anti-resonant valleys, can be greatly adjusted by suitable periodic distribution of supported masses coupled with the periodic sandwich plate.

5. Conclusions

Partial and ordinary differential coupling equations are derived from a periodic sandwich plate coupled with supported masses under random excitation. An analytical solution to the coupling equations is proposed. The frequency response characteristics and response reduction performance of the system including a sandwich plate and supported masses with various periodic geometrical and physical parameters under random support excitation are studied. The spatial periodic distributions of the layer thickness and core modulus of the sandwich plate are considered based on an active–passive periodicity strategy. The distributed masses are coupled with the plate by springs and dampers. The partial and ordinary differential coupling equations for transverse and longitudinal coupling motions of the system including the periodic sandwich plate and supported masses under random support excitation are obtained. The equations are firstly converted into unified ordinary differential equations of multi-mode coupling vibration, in which generalized stiffness, damping and mass are dependent on periodic distribution parameters and coupling stiffness and damping. Then the expressions of the frequency response function and response spectral density of the system are obtained and used for the analysis of the response characteristics of the spatially periodic parameter-varying system.

Numerical results show the following: (1) The vibration response characteristics of the sandwich plate coupled with supported masses can be improved greatly via the periodic distribution of geometrical and physical parameters; e.g., the resonant and anti-resonant amplitudes can be reduced via suitably choosing wave numbers and amplitudes of the facial layer thickness and suitably adjusting wave numbers and amplitudes of the core layer modulus. (2) The coupling stiffness between the plate and masses has great effects on the response characteristics and needs to be determined suitably, while the small coupling damping has a slight effect on the response of the sandwich plate with supported masses. (3) The periodic mass distribution (decentralization and optimized placement) can greatly improve the response characteristics of the sandwich plate and supported masses, e.g., resonant and anti-resonant amplitudes. The results on response characteristics or response reduction performance including anti-resonances have the potential for application to dynamic control or optimization of smart sandwich structures coupled with distributed masses via active–passive periodic distribution of geometrical and physical parameters. However, the analysis and experiments of active temporal control with the spatial periodic control for composite structures coupled with masses need to be developed further.

Author Contributions: Conceptualization, Z.-G.Y. and Y.-Q.N.; methodology, Z.-G.Y.; software, Z.-G.R.; validation, Z.-G.R.; writing—original draft preparation, Z.-G.R. and Z.-G.Y.; writing—review and editing, Y.-Q.N. and Z.-G.Y.; project administration, Z.-G.Y. and Y.-Q.N.; funding acquisition, Z.-G.Y. and Y.-Q.N. All authors have read and agreed to the published version of the manuscript.

Conflicts of Interest: The authors declare no conflict of interest.

Appendix A

$$\mathbf{Q} = [\mathbf{Q}_1^{\mathrm{T}} \quad \mathbf{Q}_2^{\mathrm{T}} \quad ... \quad \mathbf{Q}_{N_2}^{\mathrm{T}} \quad \mathbf{Q}_m^{\mathrm{T}} \quad]^{\mathrm{T}}, \ \mathbf{Q}_j = [q_{1j} \, q_{2j} \, ... \, q_{N_1 j}]^{\mathrm{T}}$$

$$\mathbf{Q}_m = [\overline{w}_{m1} \, \overline{w}_{m2} \, ... \, \overline{w}_{mn_a}]^{\mathrm{T}}, \ \mathbf{M} = \begin{bmatrix} \mathbf{M}_p & 0 \\ 0 & \mathbf{M}_m \end{bmatrix}$$

$$\mathbf{M}_p = \begin{bmatrix} \mathbf{M}_{11} & \mathbf{M}_{12} & ... & \mathbf{M}_{1N_2} \\ \mathbf{M}_{21} & \mathbf{M}_{22} & ... & \mathbf{M}_{2N_2} \\ \vdots & \vdots & \vdots & \vdots \\ \mathbf{M}_{N_2 1} & \mathbf{M}_{N_2 2} & ... & \mathbf{M}_{N_2 N_2} \end{bmatrix},$$

$$\mathbf{M}_{jn} = \begin{bmatrix} M_{jn,11} & M_{jn,12} & ... & M_{jn,1N_1} \\ M_{jn,21} & M_{jn,22} & ... & M_{jn,2N_1} \\ \vdots & \vdots & \vdots & \vdots \\ M_{jn,N_1 1} & M_{jn,N_1 2} & ... & M_{jn,N_1 N_1} \end{bmatrix}$$

$$\mathbf{M}_m = \mathrm{diag}\{m_{01} \, m_{02} \, ... \, m_{0n_a}\}$$

$$\mathbf{C} = \begin{bmatrix} \mathbf{C}_p + \mathbf{C}_{m1} & \mathbf{C}_{m2} \\ \mathbf{C}_{m2}^{\mathrm{T}} & \mathbf{C}_{m3} \end{bmatrix}, \ \mathbf{K} = \begin{bmatrix} \mathbf{K}_p + \mathbf{K}_{m1} & \mathbf{K}_{m2} \\ \mathbf{K}_{m2}^{\mathrm{T}} & \mathbf{K}_{m3} \end{bmatrix}$$

$$\mathbf{C}_p = \hat{\mathbf{C}} + \hat{\mathbf{C}}_{RS}, \ \hat{\mathbf{C}}_{RS} = \mathbf{E}\mathbf{L}_{rv} + \mathbf{J}\mathbf{L}_{sv}, \ \mathbf{K}_p = \hat{\mathbf{K}} + \hat{\mathbf{K}}_{RS},$$

$$\hat{\mathbf{K}}_{RS} = \mathbf{E}\mathbf{L}_{rd} + \mathbf{J}\mathbf{L}_{sd}$$

$$\mathbf{L}_{rv} = \mathbf{A}_a^{-1}\mathbf{B}_a(\mathbf{B}_b - \mathbf{A}_b\mathbf{A}_a^{-1}\mathbf{B}_a)^{-1}(\mathbf{V}_b - \mathbf{A}_b\mathbf{A}_a^{-1}\mathbf{V}_a) - \mathbf{A}_a^{-1}\mathbf{V}_a$$

$$\mathbf{L}_{rd} = \mathbf{A}_a^{-1}\mathbf{B}_a(\mathbf{B}_b - \mathbf{A}_b\mathbf{A}_a^{-1}\mathbf{B}_a)^{-1}(\mathbf{D}_b - \mathbf{A}_b\mathbf{A}_a^{-1}\mathbf{D}_a) - \mathbf{A}_a^{-1}\mathbf{D}_a$$

$$\mathbf{L}_{sv} = (\mathbf{B}_b - \mathbf{A}_b\mathbf{A}_a^{-1}\mathbf{B}_a)^{-1}(\mathbf{A}_b\mathbf{A}_a^{-1}\mathbf{V}_a - \mathbf{V}_b)$$

$$\mathbf{L}_{sd} = (\mathbf{B}_b - \mathbf{A}_b\mathbf{A}_a^{-1}\mathbf{B}_a)^{-1}(\mathbf{A}_b\mathbf{A}_a^{-1}\mathbf{D}_a - \mathbf{D}_b)$$

$$\hat{\mathbf{C}} = \begin{bmatrix} \hat{\mathbf{C}}_{11} & \hat{\mathbf{C}}_{12} & ... & \hat{\mathbf{C}}_{1N_2} \\ \hat{\mathbf{C}}_{21} & \hat{\mathbf{C}}_{22} & ... & \hat{\mathbf{C}}_{2N_2} \\ \vdots & \vdots & \vdots & \vdots \\ \hat{\mathbf{C}}_{N_2 1} & \hat{\mathbf{C}}_{N_2 2} & ... & \hat{\mathbf{C}}_{N_2 N_2} \end{bmatrix}, \ \hat{\mathbf{C}}_{jn} = \begin{bmatrix} \hat{C}_{jn,11} & \hat{C}_{jn,12} & ... & \hat{C}_{jn,1N_1} \\ \hat{C}_{jn,21} & \hat{C}_{jn,22} & ... & \hat{C}_{jn,2N_1} \\ \vdots & \vdots & \vdots & \vdots \\ \hat{C}_{jn,N_1 1} & \hat{C}_{jn,N_1 2} & ... & \hat{C}_{jn,N_1 N_1} \end{bmatrix}$$

$$\mathbf{C}_{m1} = \sum_{k=1}^{n_a} c_{0k}\mathbf{C}_m^k, \ \mathbf{C}_{m2} = [\mathbf{C}_{mp1} \, \mathbf{C}_{mp2} \, ... \, \mathbf{C}_{mpn_a}]$$

$$\mathbf{C}_m^k = \begin{bmatrix} \mathbf{C}_{11}^k & \mathbf{C}_{12}^k & ... & \mathbf{C}_{1N_2}^k \\ \mathbf{C}_{21}^k & \mathbf{C}_{22}^k & ... & \mathbf{C}_{2N_2}^k \\ \vdots & \vdots & \vdots & \vdots \\ \mathbf{C}_{N_2 1}^k & \mathbf{C}_{N_2 2}^k & ... & \mathbf{C}_{N_2 N_2}^k \end{bmatrix},$$

$$\mathbf{C}_{jn}^k = \begin{bmatrix} C_{jn,11}^k & C_{jn,12}^k & ... & C_{jn,1N_1}^k \\ C_{jn,21}^k & C_{jn,22}^k & ... & C_{jn,2N_1}^k \\ \vdots & \vdots & \vdots & \vdots \\ C_{jn,N_1 1}^k & C_{jn,N_1 2}^k & ... & C_{jn,N_1 N_1}^k \end{bmatrix}$$

$$\mathbf{C}_{mpj} = [\mathbf{C}_{mp,j1} \, \mathbf{C}_{mp,j2} \, ... \, \mathbf{C}_{mp,jN_2}]^{\mathrm{T}},$$

$$\mathbf{C}_{mp,jn} = [C_{mp,jn1} \, C_{mp,jn2} \, ... \, C_{mp,jnN_1}]$$

$$\mathbf{C}_{m3} = \mathrm{diag}\{c_{01} \, c_{02} \, ... \, c_{0n_a}\} \hat{\mathbf{K}} = \begin{bmatrix} \hat{\mathbf{K}}_{11} & \hat{\mathbf{K}}_{12} & ... & \hat{\mathbf{K}}_{1N_2} \\ \hat{\mathbf{K}}_{21} & \hat{\mathbf{K}}_{22} & ... & \hat{\mathbf{K}}_{2N_2} \\ \vdots & \vdots & \vdots & \vdots \\ \hat{\mathbf{K}}_{N_2 1} & \hat{\mathbf{K}}_{N_2 2} & ... & \hat{\mathbf{K}}_{N_2 N_2} \end{bmatrix},$$

$$\hat{\mathbf{K}}_{jn} = \begin{bmatrix} \hat{K}_{jn,11} & \hat{K}_{jn,12} & \dots & \hat{K}_{jn,1N_1} \\ \hat{K}_{jn,21} & \hat{K}_{jn,22} & \dots & \hat{K}_{jn,2N_1} \\ \vdots & \vdots & \vdots & \vdots \\ \hat{K}_{jn,N_11} & \hat{K}_{jn,N_12} & \dots & \hat{K}_{jn,N_1N_1} \end{bmatrix}$$

$$\mathbf{K}_{m1} = \sum_{k=1}^{n_a} k_{0k}\mathbf{K}_m^k, \ \mathbf{K}_{m2} = [\mathbf{K}_{mp1} \ \mathbf{K}_{mp2} \ \dots \ \mathbf{K}_{mpn_a}]$$

$$\mathbf{K}_m^k = \begin{bmatrix} \mathbf{K}_{11}^k & \mathbf{K}_{12}^k & \dots & \mathbf{K}_{1N_2}^k \\ \mathbf{K}_{21}^k & \mathbf{K}_{22}^k & \dots & \mathbf{K}_{2N_2}^k \\ \vdots & \vdots & \vdots & \vdots \\ \mathbf{K}_{N_21}^k & \mathbf{K}_{N_22}^k & \dots & \mathbf{K}_{N_2N_2}^k \end{bmatrix},$$

$$\mathbf{K}_{jn}^k = \begin{bmatrix} K_{jn,11}^k & K_{jn,12}^k & \dots & K_{jn,1N_1}^k \\ K_{jn,21}^k & K_{jn,22}^k & \dots & K_{jn,2N_1}^k \\ \vdots & \vdots & \vdots & \vdots \\ K_{jn,N_11}^k & K_{jn,N_12}^k & \dots & K_{jn,N_1N_1}^k \end{bmatrix} \mathbf{K}_{mpj} = [\mathbf{K}_{mp,j1} \ \mathbf{K}_{mp,j2} \ \dots \ \mathbf{K}_{mp,jN_2}]^{\mathrm{T}},$$

$$\mathbf{K}_{mp,jn} = [K_{mp,jn1} \ K_{mp,jn2} \ \dots \ K_{mp,jnN_1}]$$

$$\mathbf{K}_{m3} = \mathrm{diag}\{k_{01} \ k_{02} \ \dots \ k_{0n_a}\}$$

$$\mathbf{E} = \begin{bmatrix} \mathbf{E}_{11} & \mathbf{E}_{12} & \dots & \mathbf{E}_{1N_2} \\ \mathbf{E}_{21} & \mathbf{E}_{22} & \dots & \mathbf{E}_{2N_2} \\ \vdots & \vdots & \vdots & \vdots \\ \mathbf{E}_{N_21} & \mathbf{E}_{N_22} & \dots & \mathbf{E}_{N_2N_2} \end{bmatrix}, \ \mathbf{E}_{jn} = \begin{bmatrix} E_{jn,11} & E_{jn,12} & \dots & E_{jn,1N_1} \\ E_{jn,21} & E_{jn,22} & \dots & E_{jn,2N_1} \\ \vdots & \vdots & \vdots & \vdots \\ E_{jn,N_11} & E_{jn,N_12} & \dots & E_{jn,N_1N_1} \end{bmatrix}$$

$$\mathbf{J} = \begin{bmatrix} \mathbf{J}_{11} & \mathbf{J}_{12} & \dots & \mathbf{J}_{1N_2} \\ \mathbf{J}_{21} & \mathbf{J}_{22} & \dots & \mathbf{J}_{2N_2} \\ \vdots & \vdots & \vdots & \vdots \\ \mathbf{J}_{N_21} & \mathbf{J}_{N_22} & \dots & \mathbf{J}_{N_2N_2} \end{bmatrix}, \ \mathbf{J}_{jn} = \begin{bmatrix} J_{jn,11} & J_{jn,12} & \dots & J_{jn,1N_1} \\ J_{jn,21} & J_{jn,22} & \dots & J_{jn,2N_1} \\ \vdots & \vdots & \vdots & \vdots \\ J_{jn,N_11} & J_{jn,N_12} & \dots & J_{jn,N_1N_1} \end{bmatrix} \quad (\text{A1})$$

$$\mathbf{A}_\alpha = \begin{bmatrix} \mathbf{A}_{\alpha,11} & \mathbf{A}_{\alpha,12} & \dots & \mathbf{A}_{\alpha,1N_2} \\ \mathbf{A}_{\alpha,21} & \mathbf{A}_{\alpha,22} & \dots & \mathbf{A}_{\alpha,2N_2} \\ \vdots & \vdots & \vdots & \vdots \\ \mathbf{A}_{\alpha,N_21} & \mathbf{A}_{\alpha,N_22} & \dots & \mathbf{A}_{\alpha,N_2N_2} \end{bmatrix},$$

$$\mathbf{A}_{\alpha,jn} = \begin{bmatrix} A_{\alpha,jn,11} & A_{\alpha,jn,12} & \dots & A_{\alpha,jn,1N_1} \\ A_{\alpha,jn,21} & A_{\alpha,jn,22} & \dots & A_{\alpha,jn,2N_1} \\ \vdots & \vdots & \vdots & \vdots \\ A_{\alpha,jn,N_11} & A_{\alpha,jn,N_12} & \dots & A_{\alpha,jn,N_1N_1} \end{bmatrix}$$

$$\mathbf{B}_\alpha = \begin{bmatrix} \mathbf{B}_{\alpha,11} & \mathbf{B}_{\alpha,12} & \dots & \mathbf{B}_{\alpha,1N_2} \\ \mathbf{B}_{\alpha,21} & \mathbf{B}_{\alpha,22} & \dots & \mathbf{B}_{\alpha,2N_2} \\ \vdots & \vdots & \vdots & \vdots \\ \mathbf{B}_{\alpha,N_21} & \mathbf{B}_{\alpha,N_22} & \dots & \mathbf{B}_{\alpha,N_2N_2} \end{bmatrix},$$

$$\mathbf{B}_{\alpha,jn} = \begin{bmatrix} B_{\alpha,jn,11} & B_{\alpha,jn,12} & \dots & B_{\alpha,jn,1N_1} \\ B_{\alpha,jn,21} & B_{\alpha,jn,22} & \dots & B_{\alpha,jn,2N_1} \\ \vdots & \vdots & \vdots & \vdots \\ B_{\alpha,jn,N_11} & B_{\alpha,jn,N_12} & \dots & B_{\alpha,jn,N_1N_1} \end{bmatrix}$$

$$\mathbf{D}_\alpha = \begin{bmatrix} \mathbf{D}_{\alpha,11} & \mathbf{D}_{\alpha,12} & \dots & \mathbf{D}_{\alpha,1N_2} \\ \mathbf{D}_{\alpha,21} & \mathbf{D}_{\alpha,22} & \dots & \mathbf{D}_{\alpha,2N_2} \\ \vdots & \vdots & \vdots & \vdots \\ \mathbf{D}_{\alpha,N_21} & \mathbf{D}_{\alpha,N_22} & \dots & \mathbf{D}_{\alpha,N_2N_2} \end{bmatrix},$$

$$\mathbf{D}_{\alpha,jn} = \begin{bmatrix} D_{\alpha,jn,11} & D_{\alpha,jn,12} & \cdots & D_{\alpha,jn,1N_1} \\ D_{\alpha,jn,21} & D_{\alpha,jn,22} & \cdots & D_{\alpha,jn,2N_1} \\ \vdots & \vdots & \vdots & \vdots \\ D_{\alpha,jn,N_11} & D_{\alpha,jn,N_12} & \cdots & D_{\alpha,jn,N_1N_1} \end{bmatrix}$$

$$\mathbf{V}_{\alpha} = \begin{bmatrix} \mathbf{V}_{\alpha,11} & \mathbf{V}_{\alpha,12} & \cdots & \mathbf{V}_{\alpha,1N_2} \\ \mathbf{V}_{\alpha,21} & \mathbf{V}_{\alpha,22} & \cdots & \mathbf{V}_{\alpha,2N_2} \\ \vdots & \vdots & \vdots & \vdots \\ \mathbf{V}_{\alpha,N_21} & \mathbf{V}_{\alpha,N_22} & \cdots & \mathbf{V}_{\alpha,N_2N_2} \end{bmatrix},$$

$$\mathbf{V}_{\alpha,jn} = \begin{bmatrix} V_{\alpha,jn,11} & V_{\alpha,jn,12} & \cdots & V_{\alpha,jn,1N_1} \\ V_{\alpha,jn,21} & V_{\alpha,jn,22} & \cdots & V_{\alpha,jn,2N_1} \\ \vdots & \vdots & \vdots & \vdots \\ V_{\alpha,jn,N_11} & V_{\alpha,jn,N_12} & \cdots & V_{\alpha,jn,N_1N_1} \end{bmatrix}$$

$$\mathbf{F}_C = [\mathbf{F}_{C1}^{\mathrm{T}} \quad \mathbf{F}_{C2}^{\mathrm{T}} \quad \cdots \quad \mathbf{F}_{CN_2}^{\mathrm{T}} \quad \mathbf{F}_{Cm} \quad]^{\mathrm{T}}, \ \mathbf{F}_{Cj} = [F_{C,1j} F_{C,2j} \cdots F_{C,N_1j}]^{\mathrm{T}}$$

$$\mathbf{F}_{Cm} = [m_{01} \ m_{02} \cdots m_{0n_a}]^{\mathrm{T}}$$

$$\alpha = a, b$$

References

1. Ni, Y.Q.; Ying, Z.G.; Chen, Z.H. Micro-vibration suppression of equipment supported on a floor incorporating magneto-rheological elastomer core. *J. Sound Vib.* **2011**, *330*, 4369–4383. [CrossRef]
2. Stengel, R.F. *Stochastic Optimal Control: Theory and Application*; John Wiley & Sons: New York, NY, USA, 1986.
3. Housner, G.W.; Bergman, L.A.; Caughey, T.K.; Chassiakos, A.G.; Claus, R.O.; Masri, S.F.; Skelton, R.E.; Soong, T.T.; Spencer, B.F.; Yao, J.T.P. Structural control: Past, present, and future. *ASCE J. Eng. Mech.* **1997**, *123*, 897–971. [CrossRef]
4. Baleanu, D.; Sajjadi, S.S.; Asad, J.H.; Jajarmi, A.; Estiri, E. Hyperchaotic behaviors, optimal control, and synchronization of a nonautonomous cardiac conduction system. *Adv. Differ. Equ.* **2021**, *2021*, 157. [CrossRef]
5. Baleanu, D.; Sajjadi, S.S.; Jajarmi, A.; Defterli, O. On a nonlinear dynamical system with both chaotic and non-chaotic behaviors: A new fractional analysis and control. *Adv. Differ. Equ.* **2021**, *2021*, 234. [CrossRef]
6. Vaseghi, B.; Mobayen, S.; Hashemi, S.S.; Fekih, A. Fast reaching finite time synchronization approach for chaotic systems with application in medical image encryption. *IEEE Access* **2021**, *9*, 25911–25925. [CrossRef]
7. Saeed, N.A.; Awrejcewicz, J.; Alkashif, M.A.; Mohamed, M.S. 2D and 3D visualization for the static bifurcations and nonlinear oscillations of a self-excited system with time-delayed controller. *Symmetry* **2022**, *14*, 621. [CrossRef]
8. Eshaghi, M.; Sedaghati, R.; Rakheja, S. Dynamic characteristics and control of magnetorheological/electrorheological sandwich structures: A state-of-the-art review. *J. Intell. Mater. Syst. Struct.* **2016**, *27*, 2003–2037. [CrossRef]
9. Yeh, J.Y. Vibration analysis of sandwich rectangular plates with magnetorheological elastomer damping treatment. *Smart Mater. Struct.* **2013**, *22*, 035010. [CrossRef]
10. Aguib, S.; Nour, A.; Zahloul, H.; Bossis, G.; Chevalier, Y.; Lancon, P. Dynamic behavior analysis of a magnetorheological elastomer sandwich plate. *Int. J. Mech. Sci.* **2014**, *87*, 118–136. [CrossRef]
11. Babu, V.R.; Vasudevan, R. Dynamic analysis of tapered laminated composite magnetorheological elastomer (MRE) sandwich plates. *Smart Mater. Struct.* **2016**, *25*, 035006. [CrossRef]
12. Mikhasev, G.I.; Eremeyev, V.A.; Wilde, K.; Maevskaya, S.S. Assessment of dynamic characteristics of thin cylindrical sandwich panels with magnetorheological core. *J. Intell. Mater. Syst. Struct.* **2019**, *30*, 2748–2769. [CrossRef]
13. Kernytskyy, I.; Koda, E.; Diveyev, B.; Horbay, O.; Sopilnyk, L.; Humenuyk, R.; Sholudko, Y.; Osinski, P. Identification of magnetorheological layer properties by using refined plate theory. *Symmetry* **2021**, *13*, 1601. [CrossRef]
14. Hasheminejad, S.M.; Shabanimotlagh, M. Magnetic-field-dependent sound transmission properties of magnetorheological elastomer-based adaptive panels. *Smart Mater. Struct.* **2010**, *19*, 035006. [CrossRef]
15. Ying, Z.G.; Ni, Y.Q.; Ye, S.Q. Stochastic micro-vibration suppression of a sandwich plate using a magneto-rheological visco-elastomer core. *Smart Mater. Struct.* **2014**, *23*, 025019. [CrossRef]
16. Vemuluri, R.B.; Rajamohan, V.; Arumugam, A.B. Dynamic characterization of tapered laminated composite sandwich plates partially treated with magnetorheological elastomer. *J. Sandw. Struct. Mater.* **2018**, *20*, 308–350. [CrossRef]
17. Vemuluri, R.B.; Rajamohan, V.; Sudhager, P.E. Structural optimization of tapered composite sandwich plates partially treated with magnetorheological elastomers. *Compos. Struct.* **2018**, *200*, 258–276. [CrossRef]
18. Soleymani, T.; Arani, A.G. On aeroelastic stability of a piezo-MRE sandwich plate in supersonic airflow. *Compos. Struct.* **2019**, *230*, 111532. [CrossRef]
19. Hoseinzadeh, M.; Rezaeepazhand, J. Dynamic stability enhancement of laminated composite sandwich plates using smart elastomer layer. *J. Sandw. Struct. Mater.* **2020**, *22*, 2796–2817. [CrossRef]

20. Guo, Z.K.; Hu, G.; Sorokin, V.; Yang, Y.; Tang, L. Sound transmission through sandwich plate with hourglass lattice truss core. *J. Sandw. Struct. Mater.* **2020**, *23*, 1902–1928. [CrossRef]

21. Ying, Z.G.; Ni, Y.Q. Vibration localization and anti-localization of nonlinear multi-support beams with support periodicity defect. *Symmetry* **2021**, *13*, 2234. [CrossRef]

22. Jedrysiak, J. Higher order vibrations of thin periodic plates. *Thin Walled Struct.* **2009**, *47*, 890–901. [CrossRef]

23. Bisegna, P.; Caruso, G. Dynamical behavior of disordered rotationally periodic structures: A homogenization approach. *J. Sound Vib.* **2011**, *330*, 2608–2627. [CrossRef]

24. Pourasghar, A.; Chen, Z. Nonlinear vibration and modal analysis of FG nanocomposite sandwich beams reinforced by aggregated CNTs. *Polym. Eng. Sci.* **2019**, *59*, 1362–1370. [CrossRef]

25. Pourasghar, A.; Chen, Z. Effect of hyperbolic heat conduction on the linear and nonlinear vibration of CNT reinforced size-dependent functionally graded microbeams. *Int. J. Eng. Sci.* **2019**, *137*, 57–72. [CrossRef]

26. Domagalski, L.; Swiatek, M.; Jedrysiak, J. An analytical-numerical approach to vibration analysis of periodic Timoshenko beams. *Compos. Struct.* **2019**, *211*, 490–501. [CrossRef]

27. Demir, O. Differential transform method for axisymmetric vibration analysis of circular sandwich plates with viscoelastic core. *Symmetry* **2022**, *14*, 852. [CrossRef]

28. Flugge, W. *Viscoelasticity*; Springer: New York, NY, USA, 1975.